

Development of Ni/SiO₂ Nanoparticle

by

Rohaya binti Ramli

Dissertation submitted in partial fulfilment of
the requirements for the
Bachelor of Engineering (Hons)
Chemical Engineering

JULY 2009

Universiti Teknologi PETRONAS
Bandar Seri Iskandar
31750 Tronoh
Perak Darul Ridzuan

CERTIFICATION OF APPROVAL

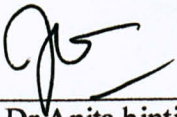
Development of Ni/SiO₂ Nanoparticle

by

Rohaya binti Ramli

A project dissertation submitted to the
Chemical Engineering Programme
Universiti Teknologi PETRONAS
in partial fulfilment of the requirement for the
BACHELOR OF ENGINEERING (Hons)
(CHEMICAL ENGINEERING)

Approved by,



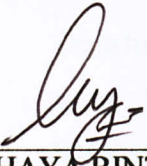
(AP Dr Anita binti Ramli)

DR ANITA binti RAMLI
Associate Professor
Fundamental & Applied Sciences Department
Universiti Teknologi PETRONAS, PERAK

UNIVERSITI TEKNOLOGI PETRONAS
TRONOH, PERAK
July 2009

CERTIFICATION OF ORIGINALITY

This is to certify that I am responsible for the work submitted in this project, that the original work is my own except as specified in the references and acknowledgements, and that the original work contained herein have not been undertaken or done by unspecified sources or persons.



(ROHAYA BINTI RAMLI)

ABSTRACT

Nanocomposite of Ni/SiO₂ was prepared by through in situ sol gel method in which Ni nanoparticles were dispersed in the silica glassy matrix. The prepared dried gel of Ni/SiO₂ at 120°C was heated to different calcination temperatures which are at 300°C, 500°C, 575°C and 600°C and identified the temperature range of the nanocomposite formation through XRD patterns.

The structure and thermal behavior of nanocomposite was identified through Fourier Transform Infrared Spectrometry (FTIR). The results of preparation also checked using Scanning Electron Microscope (SEM), Brunauer-Emmett-Teller (BET), Scanning, Thermo Gravimetric Analysis and (TGA), X-Ray Diffraction (XRD). Throughout this report will be discussed more on the structure and morphology of the particle whether it is in nanoparticle size or not and also calculating crystal size of the particle. Instead of that, in this report will be mentioned the various applications of nickel.

ACKNOWLEDGEMENT

In the name of Allah, Most Gracious and Most Merciful. Alhamdulillah, with his willing, I am able to complete my Final Year Research Project. It is a great pleasure and gratitude for me to acknowledge the people who have help, guide and support me in completing this project.

First and foremost, special thanks to my supervisor, AP Dr Anita Ramli, for being very helpful and supportive in sharing her knowledge with me. Constant support and encouragement that she gave throughout the semesters has made the project meaningful and completed successfully. I would also like to express my utmost appreciation to the chemical lab technicians, especially to Mr Fazli, Mr Jailani, Mrs Hasneyza and Miss Azimah for their assistance during the laboratory works. Not forgotten also my utmost appreciation to mechanical lab technicians especially Mr Faisal, Mr Omar as well as Mr Irwan for their assistance and willingness in analyzing my samples. I would also like to thank you to Miss Ami Salwani, is a postgraduate student who give me guidance in analyzing XRD result.

Heartfelt appreciation dedicated to my dearest mum and dad for their warmth and support throughout my journey of study in Universiti Teknologi PETRONAS. Not forgetting to all my friends and colleagues, thank you very much for your help and motivation in making this project successful and meet the objectives.

TABLE OF CONTENTS

ABSTRACT	i
CHAPTER 4: RESULTS AND DISCUSSION	21
ACKNOWLEDGEMENT	ii
CHAPTER 1: INTRODUCTION	1
1.1 Background of Study	1
1.2 Problem Statement	2
1.3 Objectives and Scope of Study	3
CHAPTER 2: LITERATURE REVIEW AND THEORY	4
2.1 Characteristics and Application of Nickel	4
2.2 Nanocomposite	5
2.3 Tetraethyl orthosilicate (TEOS)	7
2.4 Sol gel Method.	8
CHAPTER 3: METHODOLOGY	12
3.1 Sample Preparation	12
3.2 Sample Testing	15
3.2.1 BET	15
3.2.2 XRD	15

3.2.3	SEM	18
3.2.4	FTIR	19
3.2.5	TGA	20
CHAPTER 4: RESULTS AND DISCUSSION		
4.1	Data Gathering & Analysis	21
4.2	Result of Analysis	24
CHAPTER 5: CONCLUSION AND RECOMMENDATION		
5.1	Conclusion	36
5.2	Recommendations and Way Forward	36
REFERENCES		
APPENDIX		
A:	Infrared Spectroscopy	39
B:	Individual XRD Dafractogram	42

LIST OF FIGURES

Figure 2.1:	Graph of Application of Nickel	5
Figure 2.2:	Molecular structure of TEOS	7
Figure 2.3:	Schematic representation of sol-gel process of synthesis of nanomaterials	10
Figure 3.1:	XRD Equipment (Bruker AXS)	15
Figure 3.2:	Size-dependent XRD Pattern of CoPt ₃ Nano-crystals	17
Figure 3.3:	SEM Equipment	18
Figure 4.1:	Sample of Ni-SiO ₂ after forming wet gel	21
Figure 4.2:	(a) Dried green solid at 120°C overnight	22
	(b) Dried green solid after grounded	22
Figure 4.3:	(a) Sample after calcination at different temperature	22
	(b) Sample after calcination and grounded	22
Figure 4.4:	XRD Profiles	24
Figure 4.5:	Graph of Crystal Size Respect to Calcination Temperature	27
Figure 4.6:	Graph of Maximum Intensity Respect to Calcination Temperature	28
Figure 4.7:	The Morphology of Ni/SiO ₂ for 0.1 mol (NO ₃) ₂ .6H ₂ O	29
Figure 4.8:	The Morphology of Ni/SiO ₂ for 0.5 mol (NO ₃) ₂ .6H ₂ O	30
Figure 4.9:	Graph of TGA Analysis for 0.1 mol Ni	31
Figure 4.10:	Graph of TGA Analysis for 0.5 mol Ni	32
Figure 4.11:	IR Spectra on Ni/SiO ₂ for 0.1 mol Ni	33

LIST OF TABLES

Table 4.1: Crystal System of the Compound	25
Table 4.2: Crystal Size for Sample 0.1 mol Ni	26
Table 4.3: Crystal Size for Sample 0.5 mol Ni	26
Table 4.4: Maximum Intensity Respect to Calcination Temperature	27
Table 4.5: Functional Groups of Compound	35

CHAPTER 1

INTRODUCTION

1.1 Background of Study

Materials with nanometer size particles exhibit unique chemical and physical properties. In particular, nanoparticle materials composed of nanometric metal and metal oxide particles embedded in vitreous matrices, present a variety of interesting magnetic, electric and catalytic properties that are strongly size-dependent. The nanoparticle which has been studied is Ni/SiO₂ at different compositions. These nanoparticles are a class of magnetic nanoparticles which using magnetic field commonly consist of magnetic elements such as iron, nickel and cobalt and their chemical compounds. These particles have been the focus of much research recently because they possess attractive properties which could see potential use in catalysis, biomedicine, magnetic resonance imaging, data storage and environmental remediation. These elements are dispersed on a silica support. Silica-supported nickel catalyst is among the most well known catalyst used for hydrogenation, hydrogenolysis and methane reforming reactions [Morikawa et. al]. The dispersion of metallic particles in SiO₂ glassy matrix materials gives rise to materials in which the electric resistivity varies with metal content and a transition from the metallic to the insulating regime and improved its properties such as thermal stability and hardness.

There are several traditional preparation methods that have been investigated to produce catalyst and also nanoparticle which are impregnation, deposition-precipitation, and metallic ion exchange. Recently, several techniques have been proposed such as reduction of metal using alkaline metals, evaporation-condensation, partial recrystallization of amorphous materials and also sol-gel technique. Most of the works, the catalysts are prepared by impregnation and ion exchange methods.

However, it is difficult to increase the dispersion of Ni in Ni/SiO₂, particularly at high Ni loading because fine Ni particles easily aggregate during calcinations [Takahashi et al]. We used sol gel technique to prepare Ni/SiO₂ nanoparticle since it has many advantages over other methods like low temperature processing, high chemical homogeneity, purity, allows obtaining materials with high BET areas and controlling the porosity. From chemical point of view, sol gel method depends on many parameters that make it difficult to control the process and reproducibility. The structural properties of Ni/SiO₂ nanoparticle have been investigated.

1.2 Problem Statement

Although the hydrogenation of Natural Oils reaction can be catalyzed by many metals, nickel is most commonly used for three important practical reasons: low cost, good catalytic activity and metal inertness [Gian Paolo et al]. The main problems associated with the use of Ni catalysts are the low selectivity and the high activity for isomerization reactions. The activity is determined by the Ni surface and its accessibility, which also affects the selectivity of the process. Thus the activity phase is usually dispersed on a solid support, which also acts as a filter aid and even as promoter. Kieselguhr is the most used support. Improvements in supports have been made; synthetic silica or silicates have shown better catalyst reproducibility from batch to batch, with an increase in surface area and a decrease of mean particle size. Many impurities in the feed stocks may act as poisons for nickel catalysts. Oxygenated products (including water, free fatty acids and oxidized fats) and sulfur compound inhibit the ability of Ni to adsorb H₂; this then favors the isomerization reactions. Phosphorous compounds are large enough block pores, with a consequent reduction in catalytic activity. For this reason the feed stocks are now being increasingly purified to allow a reduction in the amount of catalyst needed. This makes re-use of a nickel catalyst economically unattractive. Although other catalysts, including copper and palladium have been considered, they have problems such as sensitivity to poisons.

When searching for suitable catalysts for the hydrogenation of a particular compound, one has to compromise for example selectivity and activity. For instance, certain catalyst characteristic such as open pore structure may favor the selective hydrogenation of fatty oils while at the same time result in longer reaction times when hydrogenating more contaminated oils because of their higher possibility to poisoning [Berben et al, 2009].

1.2 Characteristics and Application of Nickel

From Sciencedaily, January 2009, UC Riverside chemists have designed a catalyst to accelerate a chemical reaction that allows hydrogenated oils to be made while minimizing the production of trans-fat. Trans-fats are found in vegetable shortenings, some margarines, crackers, cookies and snacks. People are recommended to reduce their consumption of trans-fats. Hydrogenation is a process where hydrogen is added to natural oils to prolong the shelf life of foods. But, hydrogenation also results in the production of trans-fats, which have adverse health effects such as raising bad cholesterol and increasing the risk for coronary heart disorders.

1.3 Objectives and Scope of Study

There are three main objectives of this research which are:

- i. To increase the surface area of Ni by entrapping within porous network using sol gel method
- ii. To study on physical and chemical properties of Ni/SiO₂ nanoparticle specifically on crystal size and morphology
- iii. To determine the suitable temperature for Ni/SiO₂ nanoparticle can be formed

CHAPTER 2

LITERATURE REVIEW & THEORY

2.1 Characteristics and Application of Nickel

Nickel is a silvery-white metal with a slight golden tinge that takes a high polish which is one of only four elements that are magnetic at or near room temperature. It is hard and ductile and belongs to the transition metals. Most often it combines with sulfur and iron in pentlandite, with sulfur in millerite, with arsenic in the mineral nickeline, with arsenic and sulfur in nickel galena. Nickel is a very reactive element, but due to formation of protective oxide surface, it is slow to react in air at normal temperatures and pressures. Nickel is chiefly valuable for the alloys especially many superalloys, and particularly stainless steel. Nickel is also a naturally magnetostrictive material which in the presence of a magnetic field, the material undergoes a small change in length. Nickel (Ni) is corrosion-resistant, finding many uses in alloys, a plating, in the manufacture of coins, magnets and common household utensils and also as a catalyst for hydrogenation.

Nickel is used in many industrial and consumer products, including stainless steel, magnets, coinage, rechargeable batteries, electric guitar strings and special alloys. It is also used for plating and as a green tint in glass. It is widely used in many other alloys, such as nickel brasses and bronzes, and alloys with copper, chromium, aluminum, lead, cobalt, silver, and gold. Nickel(III) oxide is also used as the cathode in many rechargeable batteries, including nickel-cadmium, nickel-iron, nickel hydrogen, and nickel-metal hydride, and used by certain manufacturers in Li-ion batteries.

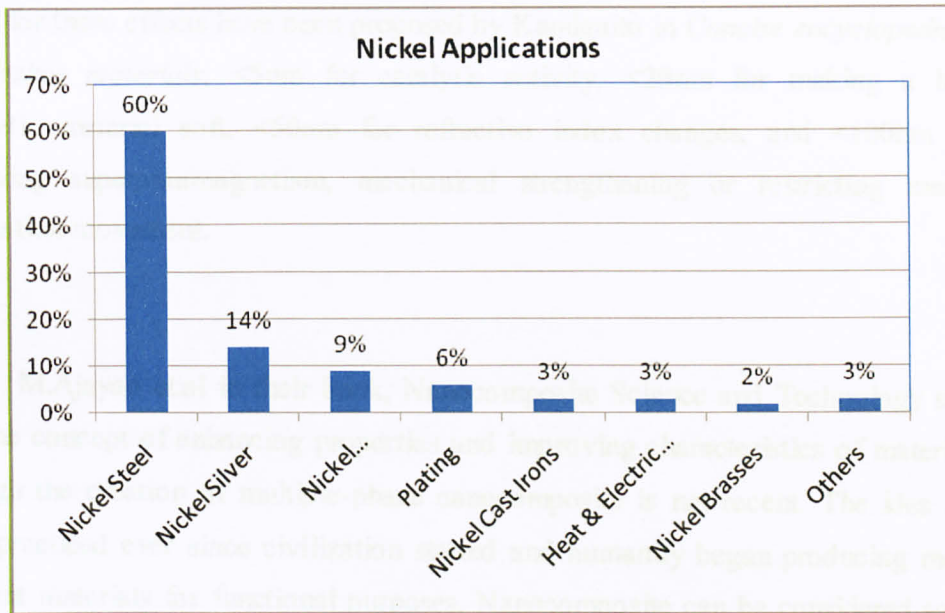


Figure 2.1: Application of Nickel

The bar chart in Figure 2.1 above shows various applications of nickel. Nickel is also frequently used as a catalyst for hydrogenation, most often using Raney nickel, a finely divided form of the metal alloyed with aluminum which adsorbs hydrogen gas [Lenntech].

2.2 Nanocomposite

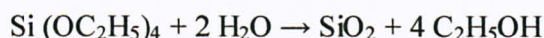
According to *Nanocomposite Science and Technology Book*, nanocomposite can be defined as multiphase solid materials where one of the phases has a dimension of less than 100 nanometers (nm): structures having nanometer scale dimensional repeat distances between the different phases that make up the material. In the broadest sense, the nanocomposite can be included as porous media, colloids, gels and copolymers, but is more usually taken to mean the solid combination of nano-dimensional phases differing in properties due to dissimilarities in structure and chemistry. The mechanical, electrical, optical, electrochemical, catalytic properties of the nanocomposite will differ markedly from that of the component materials. Size

limits for these effects have been proposed by Kamigaito in *Concise encyclopedia of composites materials*; <5nm for catalytic activity, <20nm for making a hard magnetic material soft, <50nm for refractive index changes, and <100nm for achieving superparamagnetism, mechanical strengthening or restricting matrix dislocation movement.

M.Ajayan et.al in their book, *Nanocomposite Science and Technology* said that the concept of enhancing properties and improving characteristics of materials through the creation of multiple-phase nanocomposite is not recent. The idea has been practiced ever since civilization started and humanity began producing more efficient materials for functional purposes. Nanocomposite can be considered solid structures with nanometer scale dimensional repeat distances between the different phases that constitute the structure. The materials typically consist of inorganic (host) solid containing an organic component or vice versa. Or they can consist of two or more inorganic/organic phases in some combinatorial form with the constraint that at least one of the phases or features is in nanosize. Extreme examples of nanocomposite can be in porous media, colloids, gels and copolymers. Apart from properties of individual components in a nanocomposite, interfaces play an important role in enhancing or limiting the overall properties of the system. Due to high surface area of nanostructures, nanocomposite presents many interfaces between the constituent intermixed phases (Publickel M.Ajayan, 2003).

2.3 Tetraethyl orthosilicate (TEOS)

Tetraethyl orthosilicate (TEOS) is the chemical compound with the formula $\text{Si}(\text{OC}_2\text{H}_5)_4$. Often abbreviated TEOS, this molecule consists of four ethyl groups attached to SiO_4^{4-} ion, which is called orthosilicate. As an ion in solution, orthosilicate does not exist. Alternatively TEOS can be considered to be the ethyl ester of orthosilicic acid, $\text{Si}(\text{OH})_4$. It is a prototypical alkoxide. TEOS has the remarkable property of easily converting into silicon dioxide. This reaction occurs upon the addition of water:



This hydrolysis reaction is an example of a sol-gel process. The side product is ethanol. The reaction proceeds via a series of condensation reactions that convert the TEOS molecule into a mineral-like solid via the formation of Si-O-Si linkages. Rates of this conversion are sensitive to the presence of acids and bases, both of which serve as catalysts. TEOS is widely used in many applications as silica support in preparing catalyst for example preparation nanocomposite of $\text{NiAl}_2\text{O}_4/\text{SiO}_2$ (NAS) through insitu sol-gel method which TEOS as precursor SiO_2 glassy matrix [Muralidharan et al]. Nanocomposites materials can be obtained by controlling both the size and polydispersity of the particles in the host matrix through sol-gel method where this method gives low temperature processing, high chemical homogeneity and purity.

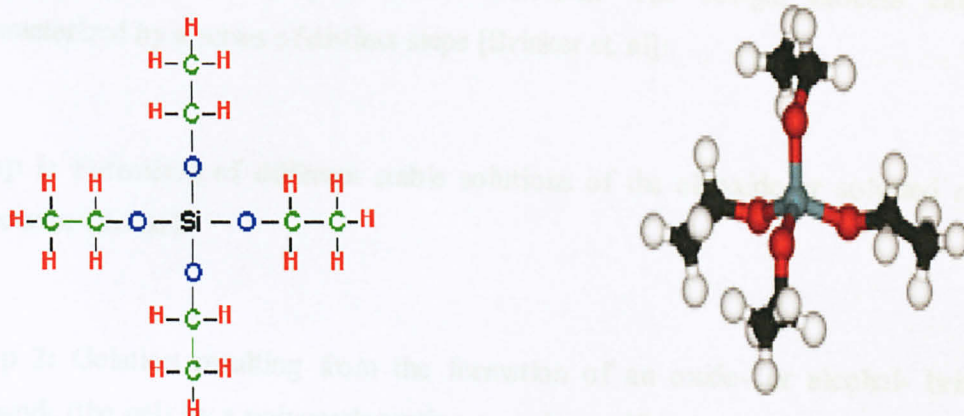


Figure 2.2: Molecular structure of TEOS

2.4 Sol gel Method

The sol-gel process involves the evolution of inorganic networks through the formation of a colloidal suspension (**sol**) and gelation of the sol to form a network in a continuous liquid phase (**gel**). The precursors for synthesizing these colloids consist usually of a metal or metalloid element surrounded by various reactive ligands. The starting material is processed to form a dispersible oxide and forms a sol in contact with water or dilute acid. Removal of the liquid from the sol yields the gel, and the sol/gel transition controls the particle size and shape. Calcination of the gel produces the oxide.

Sol-gel processing refers to the hydrolysis and condensation of alkoxide-based precursors such as $\text{Si}(\text{OEt})_4$ (tetraethyl orthosilicate, or TEOS). The reactions involved in the sol-gel chemistry based on the hydrolysis and condensation of metal alkoxide $\text{M}(\text{OR})_z$ can be described as follows:



Sol-gel method of synthesizing nonmaterial is very popular amongst chemists and is widely employed to prepare oxide materials. The sol-gel process can be characterized by a series of distinct steps [Brinker et. al]:

Step 1: Formation of different stable solutions of the alkoxide or solvated metal precursor (the sol).

Step 2: Gelation resulting from the formation of an oxide- or alcohol- bridged network (the gel) by a polycondensation or polyesterification reaction that results in a dramatic increase in the viscosity of the solution.

Step 3: Aging of the gel (Syneresis), during which the polycondensation reactions continue until the gel transforms into a solid mass, accompanied by contraction of the gel network and expulsion of solvent from gel pores. The aging process of gels can exceed 7 days and is critical to the prevention of cracks in gels that have been cast.

Step 4: Drying of the gel, when water and other volatile liquids are removed from the gel network. This process is complicated due to fundamental changes in the structure of the gel. The drying process has itself been broken into four distinct steps: (i) the constant rate period, (ii) the critical point, (iii) the falling rate period, (iv) the second falling rate period.

If isolated by thermal evaporation, the resulting monolith is termed a *xerogel*. If the solvent (such as water) is extracted under supercritical or near super critical conditions, the product is an *aerogel*.

Step 5: Dehydration, during which surface- bound M-OH groups are removed, there by stabilizing the gel against rehydration. This is normally achieved by calcining the monolith at temperatures up to 800°C.

Step 6: Densification and decomposition of the gels at high temperatures ($T > 800^{\circ}\text{C}$). The pores of the gel network are collapsed, and remaining organic species are volatilized. The typical steps that are involved in sol-gel processing are shown in the schematic diagram in Figure 2.3

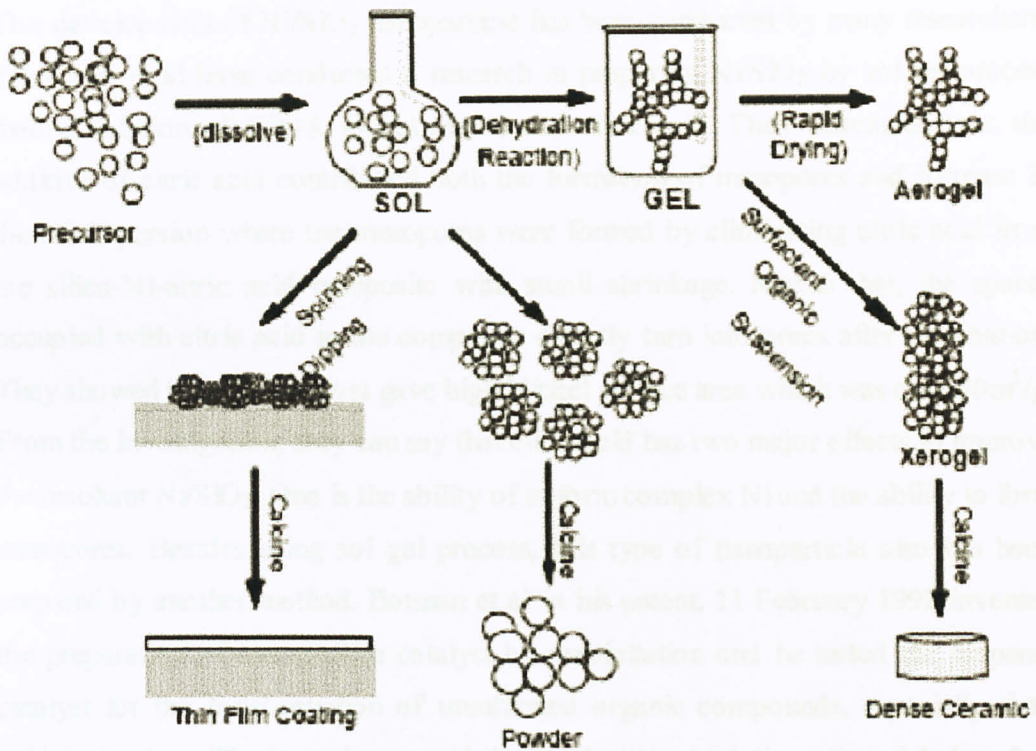


Figure 2.3: Schematic representation of sol-gel process of synthesis of nonmaterial.

Here some advantages of Sol-Gel Technique:

1. Can produce thin bond-coating to provide excellent adhesion between the metallic substrate and the top coat.
2. Can produce thick coating to provide corrosion protection performance.
3. Can easily shape materials into complex geometries in a gel state.
4. Can produce high purity products because the organo-metallic precursor of the desired ceramic oxides can be mixed, dissolved in a specified solvent and hydrolyzed into a sol, and subsequently a gel, the composition can be highly controllable.
5. Can have low temperature sintering capability, usually 200-600°C.
6. Can provide a simple, economic and effective method to produce high quality coatings.

This development of Ni/SiO₂ nanoparticle has been conducted by many researchers. Takahashi et al have conducted a research in preparing Ni/SiO₂ by sol gel process from a solution of TEOS, nickel nitrate and citric acid. They concluded that, the additive of citric acid contributed both the formation of mesopores and increase in the Ni dispersion where the mesopores were formed by eliminating citric acid from the silica-Ni-nitric acid composite with small shrinkage. Means that, the spaces occupied with citric acid in the composite directly turn into pores after elimination. They showed that, the catalyst gave high Nickel surface area which was over 30m²/g. From the investigation; they can say that citric acid has two major effects to improve the resultant Ni/SiO₂. One is the ability of to form complex Ni and the ability to form mesopores. Besides using sol gel process, this type of nanoparticle also has been prepared by another method. Botman et al in his patent, 11 February 1992 invented the preparation of nickel/silica catalyst by precipitation and he tested the prepared catalyst for the hydrogenation of unsaturated organic compounds, especially fatty acid derivatives. The invention provided a catalyst in which the active nickel surface area is above 120 m²/g nickel also has a pore volume of at least 0.35 ml/g.

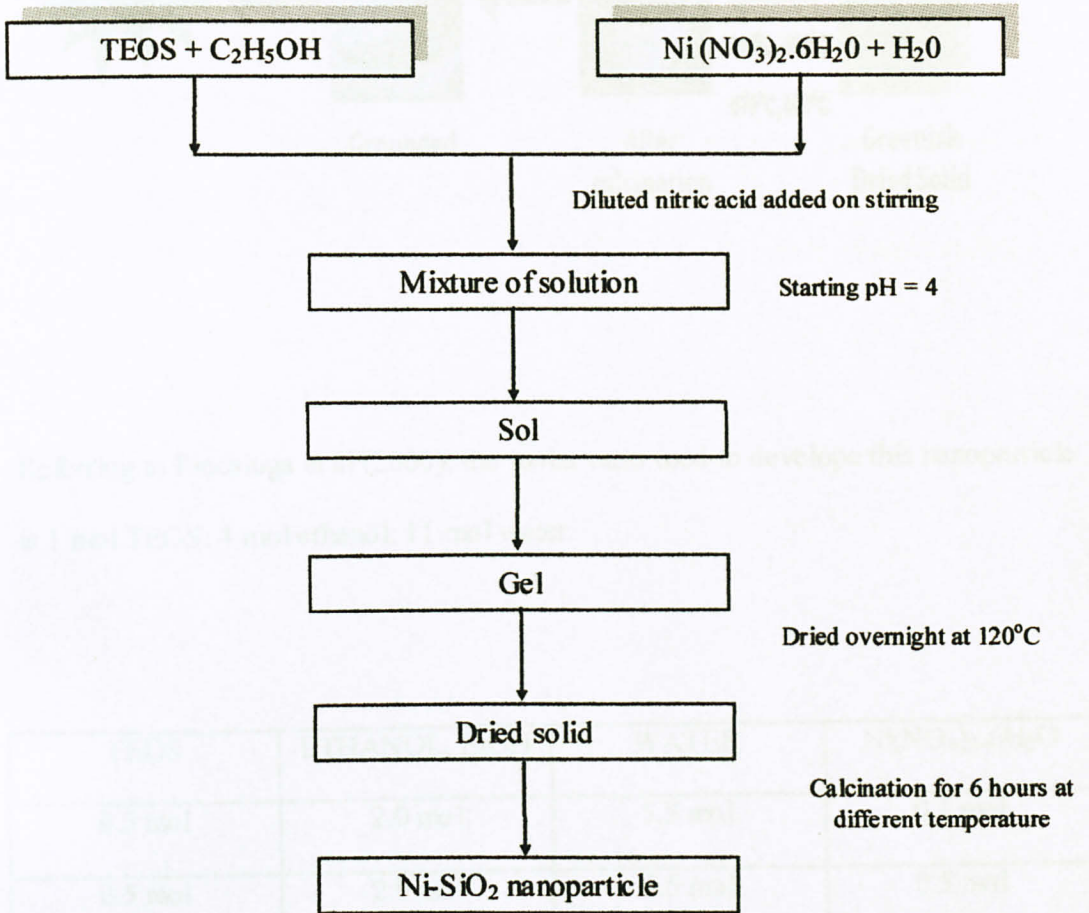


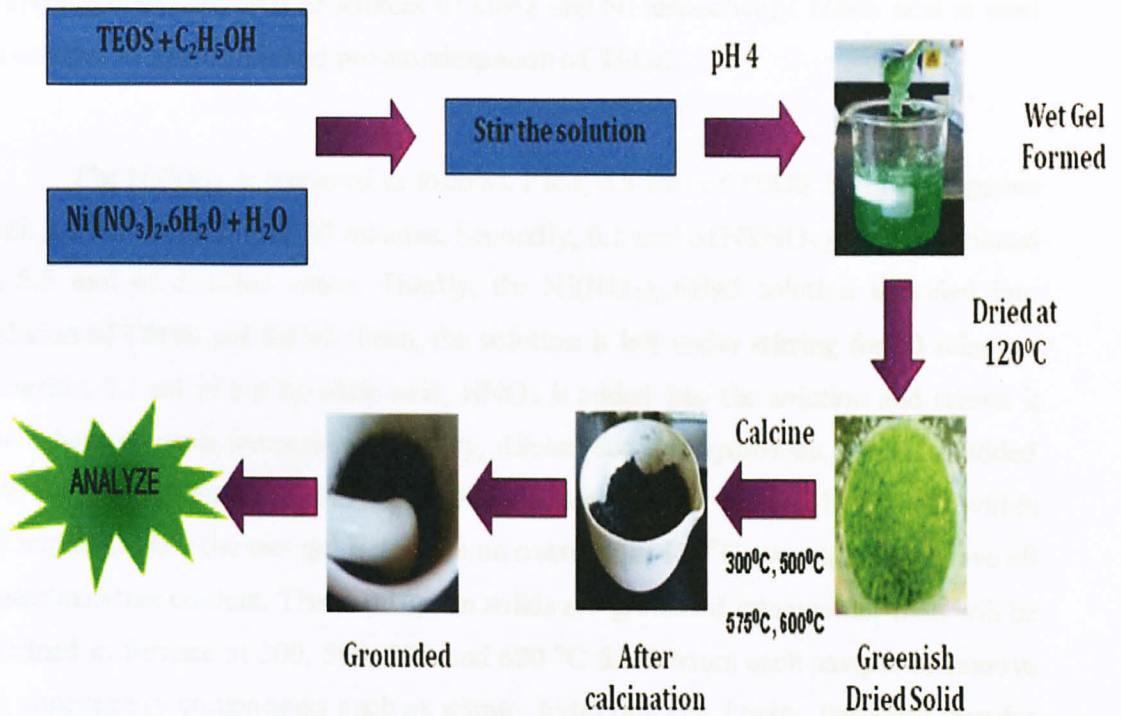
CHAPTER 3

METHODOLOGY

3.1 Sample Preparation

This methodology is referred from Cherifi et al (1997) and Piccaluga et al (2000) with some modifications.





Referring to Piccaluga et al (2000), the molar ratio used to develop this nanoparticle is 1 mol TEOS: 4 mol ethanol: 11 mol water.

TEOS	ETHANOL, EtOH	WATER	Ni(NO ₃) ₂ ·6H ₂ O
0.5 mol	2.0 mol	5.5 mol	0.1 mol
0.5 mol	2.0 mol	5.5 mol	0.5 mol

Tetraethylorthosilicate (TEOS) and nickel nitrate hexahydrate, $\text{Ni}(\text{NO}_3)_2 \cdot 6\text{H}_2\text{O}$ are used as sources of silica and Ni respectively. Nitric acid is used as catalyst in hydrolysis and polycondensation of TEOS.

The Ni/SiO_2 is prepared as follows. First, 0.5 mol of TEOS is stirred together with 2.0 mol of EtOH for 30 minutes. Secondly, 0.1 mol of $\text{Ni}(\text{NO}_3)_2 \cdot 6\text{H}_2\text{O}$ is diluted in 5.5 mol of distilled water. Thirdly, the $\text{Ni}(\text{NO}_3)_2 \cdot 6\text{H}_2\text{O}$ solution is added into solution of TEOS and EtOH. Then, the solution is left under stirring for 30 minutes. Fourthly, 0.1 ml of 3.5 M nitric acid, HNO_3 is added into the solution and stirred it for 1 hour at room temperature. Fifthly, diluted sodium hydroxide, NaOH is added into the solution until the pH reach 4. After adding NaOH, gel will be formed within 30 minutes. Then the wet gel is dried in an oven under 120°C overnight to remove all water/moisture content. The dried green solids are grounded into powder then will be calcined in furnace at 300, 500, 575 and 600°C for 6 hours each sample to remove all unnecessary components such as nitrate, hidroxide etc. Lastly, the black powder of Ni/SiO_2 is sent to FTIR, BET, TGA, XRD and SEM to analyze its characteristics.



Figure 1.1: XRD Equipment Model A1

3.2 Sample Testing

For catalyst characterization, there will be five methods being used which are Brunauer-Emmett-Teller (BET) model, X-ray Diffraction (XRD) method, and Scanning Electron Microscopy (SEM) method, Fourier Transform Infrared Spectrometry (FTIR) and Thermo Gravimetric Analysis (TGA).

3.2.1 BET

The BET model is used to determine the specific surface area of solids. But, this method is limited to meso- and macro porous solids. The interpretation of adsorption-desorption isotherms from BET procedure provides a useful information regarding the texture of the adsorbent. The main parameters that can be assessed are specific surface area, pore distribution, specific porous volume and information on structure such as pore shape as well as interconnection (John Lynch, 2003).

3.2.2 X-ray Diffraction (XRD)

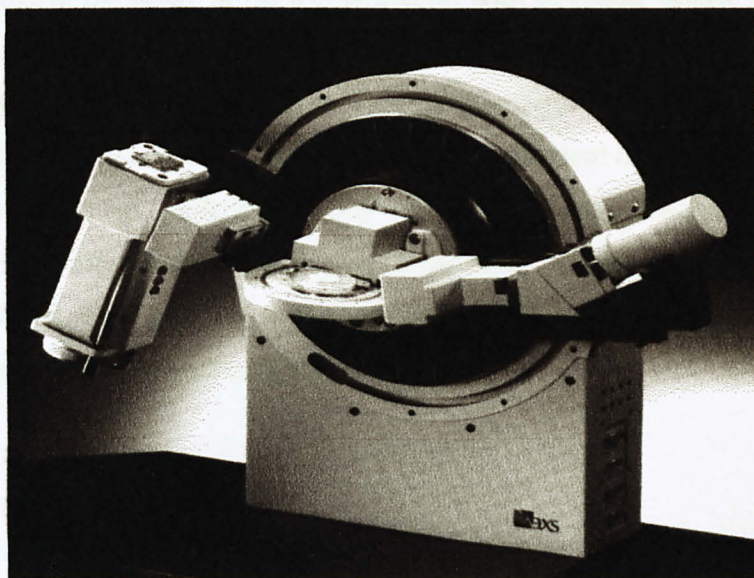


Figure 3.1: XRD Equipment (Bruker AXS)

In XRD, diffraction occurs when a sample is irradiated with electromagnetic radiation, in this case X-rays, and there is interaction with a structure where the repeat distance is on the same order as the wavelength of the electromagnetic radiation. The wavelengths of X-rays are angstroms in magnitude, which is in the range of the repeat distance in most crystalline solid materials. Diffraction occurs based on Bragg's law, which is shown in Equation below, where n is an integer, λ is the wavelength, d is the repeat distance, and θ is the angle of diffraction.

$$n\lambda = d \sin \theta$$

The output from XRD analysis yields a plot, which shows intensity versus diffraction angle, as shown in Figure 3.2. From this one can determine the crystallographic planes that are being diffracted and since the wavelength and diffraction angle is known, using Bragg's law the repeat distance, d , can be calculated, which can be utilized to create a map of the crystal structure. Alternatively, a collection of standards can be utilized to compare the peaks in the diffractogram with literature values, allowing one to identify crystal planes. Furthermore, the equipment can be configured to have a detector to measure X-ray absorption. This detector has been utilized in the work of Hormes et al. Each element has a unique absorption spectrum so utilizing X-ray diffraction and absorption elemental identification is obtained as well as the repeat distance. Schevchenko et al, utilized XRD in order to evaluate peak broadening with size decrease and their results are shown in Figure 3.2.

The information that can we get from XRD pattern is:

- Peak position
- Dimension of the elementary cell
- Peak intensity
- Content of the elementary cell
- Peak broadening
- Strain/crystallite size
- Scaling factor
- Quantitative phase amount
- Diffuse background
- False order
- Modulated background
- Close order

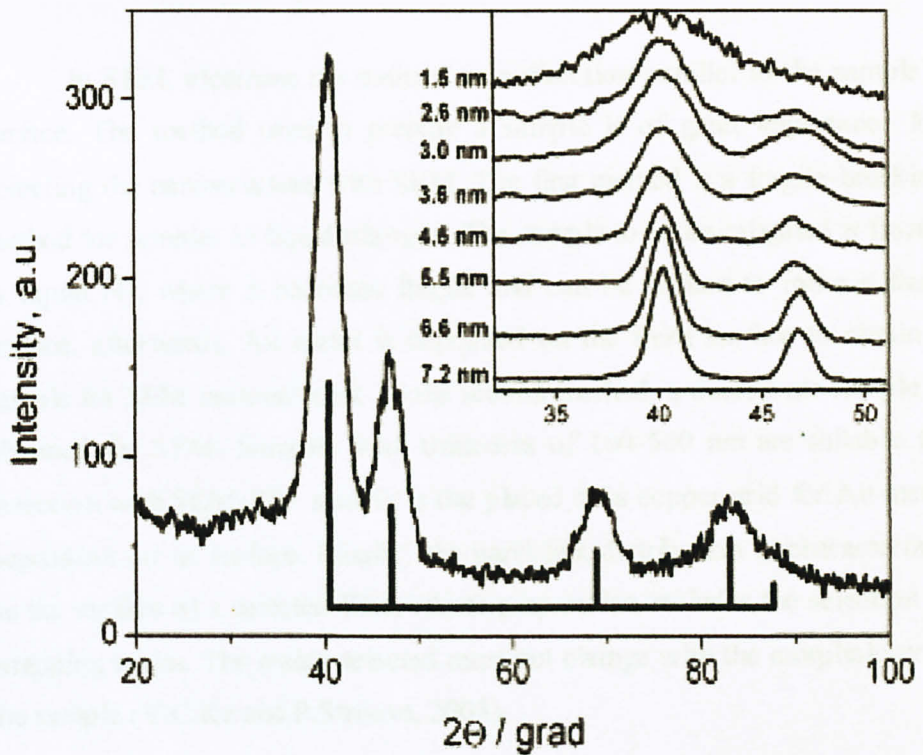


Figure 3.2: Example of size-dependent XRD Pattern of CoPt₃ Nano-crystals

3.2.3 Scanning Electron Microscopy (SEM)

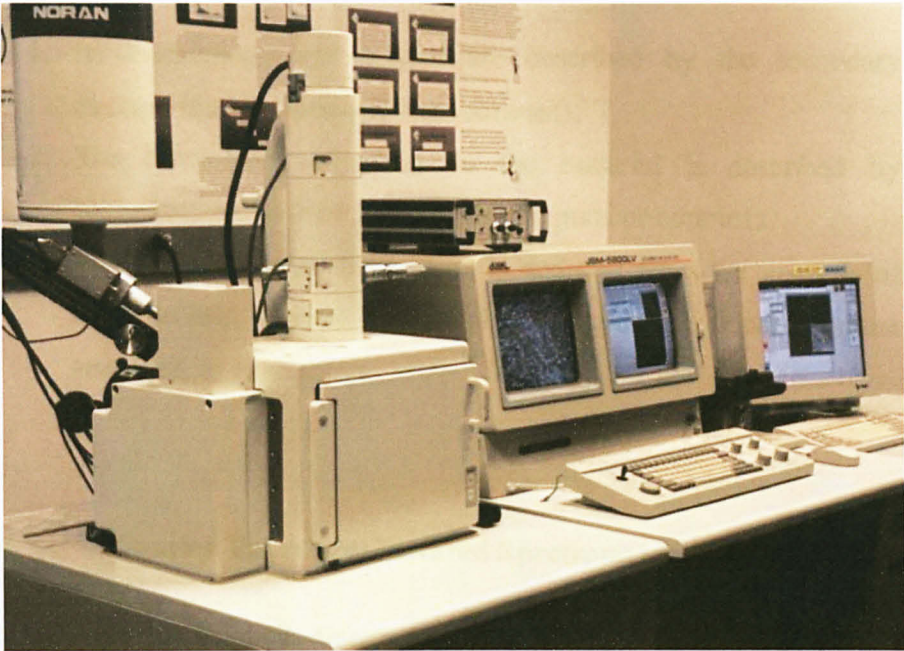


Figure 3.3: SEM Equipment

In SEM, electrons are emitted in a direction parallel to the sample's surface. The method used to prepare a sample is of great importance for detecting the nanostructure with SEM. The first method is a fragile-breaking method for samples in liquid nitrogen. The sample to be investigated is frozen in liquid N_2 , where it becomes fragile and can be broken to make a fresh surface, afterwards, Au metal is deposited on the fresh surface to obtain a sample for SEM measurement. In the second method, a microtome sample is obtained for SEM. Samples with thickness of 100-500 nm are suitable for detection with SEM. The sample is placed on a copper grid for Au metal deposition on its surface. Finally, the particle's distribution is characterized on the surface of a selected film, whose preparation includes the selection of wrapping resins. The resins selected must not change with the morphology of the sample (Y.C.Ke and P.Stroeve, 2005).

Depend on the signal used; the information extracted reveals a different property of the material (John Lynch, 2003):

1. Its morphology and texture are described by the secondary electron images (topographical contrast).
2. The distribution of phase in the material is described by backscattered electron images (atomic number contrast).
3. The composition of the phases is deduced from the analysis of characteristic X-rays emitted by the sample (local element analysis).

3.2.4 Fourier Transform Infrared Spectrometry (FTIR)

Fourier Transform Infrared Spectroscopy (FTIR) is a non-destructive analytical technique used to identify mainly organic materials. FTIR analysis results in absorption spectra which provide information about the chemical bonds and molecular structure of a material. The technique works on the fact that bonds and groups of bonds vibrate at characteristic frequencies. A molecule that is exposed to infrared rays absorbs infrared energy at frequencies which are characteristic to that molecule. During FTIR analysis, a spot on the specimen is subjected to a modulated IR beam. The specimen's transmittance and reflectance of the infrared rays at different frequencies is translated into an IR absorption plot consisting of reverse peaks. The resulting FTIR spectral pattern is then analyzed and matched with known signatures of identified materials in the FTIR library. Single fibers or particles are sufficient enough for material identification through FTIR analysis. Organic contaminants in solvents may also be analyzed by first separating the mixture into its components by gas chromatography, and then analyzing each component by FTIR.

3.2.5 Thermo Gravimetric Analysis (TGA)

TGA is a type of testing that is performed on samples to determine changes in weight in relation to change in temperature. Such analysis relies on a high degree of precision in three measurements: weight, temperature, and temperature change. As many weight loss curves look similar, the weight loss curve may require transformation before results may be interpreted. A derivative weight loss curve can be used to tell the point at which weight loss is most apparent. Again, interpretation is limited without further modifications and disconsolation of the overlapping peaks may be required. Analysis is carried out by raising the temperature gradually and plotting weight against temperature. The temperature in many testing methods routinely reaches 1000°C or greater, but the oven is so greatly insulated that an operator would not be aware of any change in temperature even if standing directly in front of the device. After the data is obtained, curve smoothing and other operations may be done such as to find the exact points of inflection (John Lynch, 2003).



Figure 1: Sample of TGA data after initial weight

CHAPTER 4

RESULT AND DISCUSSION

4.1 Data Gathering & Analysis

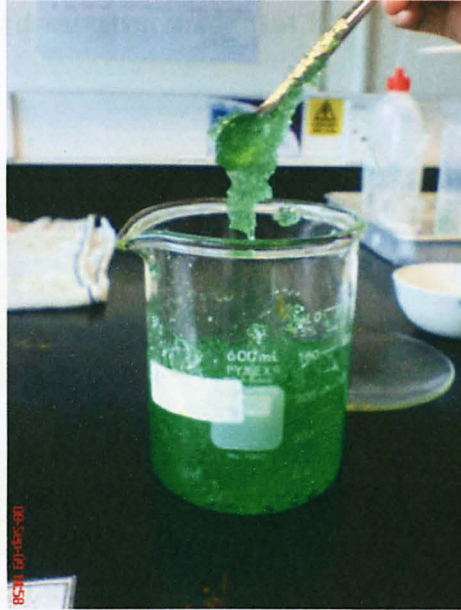


Figure 4.1 : Sample of Ni/SiO₂ after forming wet gel

Solution of nickel nitrate was added into TEOS which is hydrolyzed by ethanol at molar ratio TEOS/EtOH/water: 1/4/11. The solution was stirred for 30 minutes at room temperature with rapid mixing rate. Initially the pH of the solution; consists of Ni(NO₃)₂.6H₂O, water, ethanol and TEOS is about 3. After adding a few drops of 3.5M HNO₃ the solution is stirred for 60 minutes and pH drops to about 1.5. To maintain pH at 4 as stated in literature (Piccaluga et al) base solution; sodium hydroxide, NaOH was added until pH of the solution reached 4. From literature, gelation will occur within 2 days at room temperature but within 30 minutes stirring at pH = 4, wet gel was formed. From some studies, the gel occurs faster due to adding of NaOH and without adding NaOH solution; gel will form within 2 days.

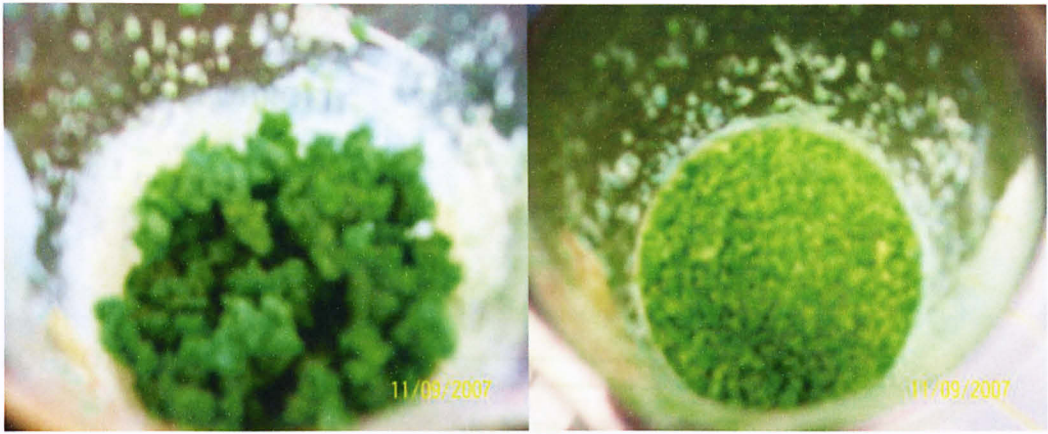


Figure 4.2: Sample for dried green solid (a) at 120°C overnight, (b) after grounded

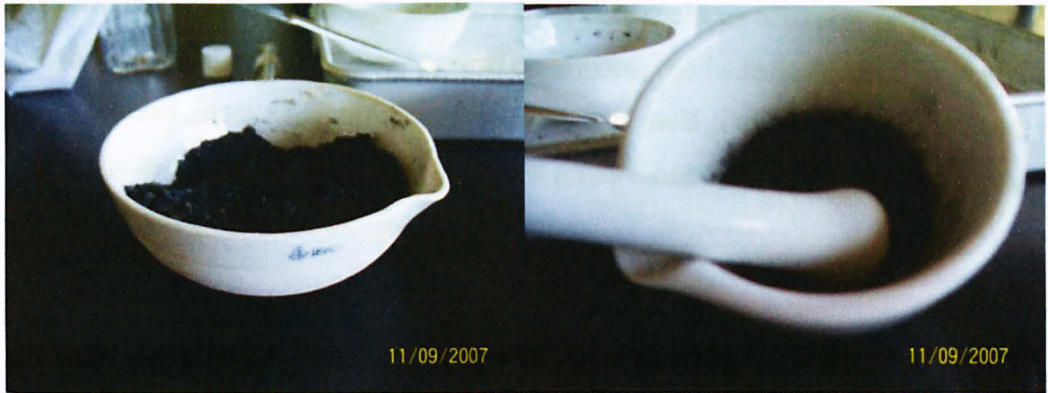
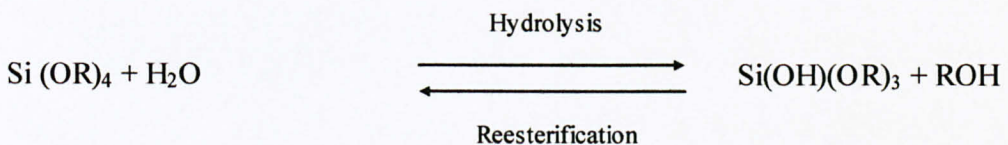
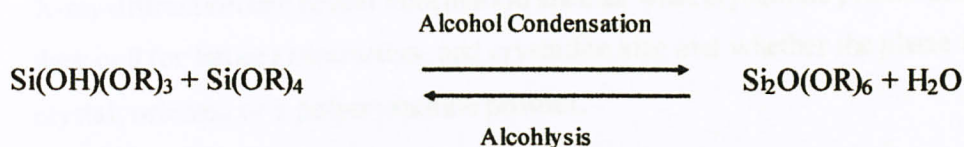
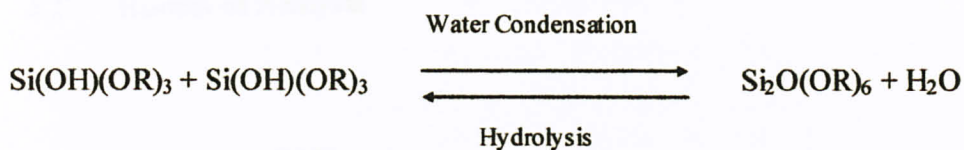


Figure 4.3: Sample after Calcination (a) at different temperature for 6 hours, (b) after grounded

For my project, the preparation of nanoparticles which are dispersed in TEOS (as precursor) so, so the nanoparticles can be coated by amorphous silica obtained from gelation of alkoxide. The fundamental reactions that take place during sol-gel process are showed below:





The hydrolysis reaction, through addition of water, replaces alkoxide groups (OR) with hydroxyl groups (OH). Under normal conditions, the hydrolysis reaction is very slow. It is most rapid and complete when catalyst (acid and base) are employed. Normally, base-catalyzed hydrolysis proceeds much more slowly than acid-catalyzed hydrolysis at an equivalent catalyst concentration.

Apart from pH, others parameters that can influence the gelation process and formation of the final products are: composition of starting solution, method of mixing the reagents, gelation temperature, gel aging, heat treatment methods, rate of solvent elimination and maximum temperature of heat treatment (Piccaluga et al, 2000).

4.2 Results of Analysis

X-Ray Diffraction (XRD)

X-ray diffraction can reveal information such as what crystalline phases are present, their cell (or lattice) parameters, and crystallite size and whether the phase is single crystal, oriented or a polycrystalline powder.

As shown in Figure 4.4, a clear XRD patterns exhibit peaks corresponding to typical NiO/SiO₂ after 6h calcinations temperatures 300°C, 500 °C, 575 °C and 600 °C. The highest intensity was obtained at about 43° of the 2θ as the major peak for all the samples. It can be observed from Table 4.4 that the highest intensity was achieved by NiO at 300°C for 0.1 mol Ni and at 500°C for 0.5 mol Ni. The intense sharp peak indicated that the well-crystalline single phase of NiO was successfully formed. This indicates that the sintering process had caused the atom to move to its own lattice completely. In appendix B, shows the individual diffractogram.

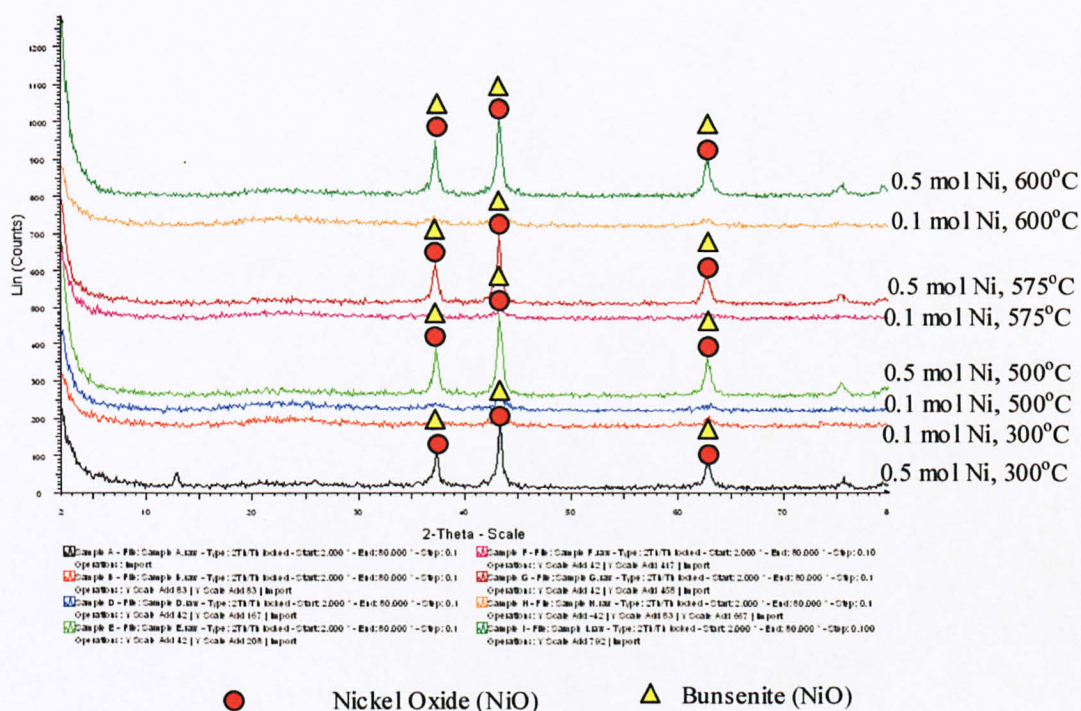


Figure 4.4: XRD Profiles of Samples at Different Molar Ratio and Calcination Temperature

XRD analysis reveals the crystal system of the compound at the highest intensity as shown below in Table 1. Most of Bunsenite compound is cubic system where $\alpha = \beta = \gamma = 90$ and for Nickel Oxide is hexagonal system where $\alpha = \beta \neq \gamma$

Table 4.1: Crystal System of the Compound

Sample Name	Compound Name	Formula	System	alpha α	beta β	gamma γ
0.1 mol Ni (300°C)	Bunsenite, syn	NiO	Cubic	90	90	90
	Nickel Oxide	NiO	Cubic	90	90	90
0.5 mol Ni (300°C)	Bunsenite, syn	NiO	Cubic	90	90	90
	Nickel Oxide	NiO	Hexagonal (Rh)	90	90	120
0.1 mol Ni (500°C)	Bunsenite, syn	NiO	Cubic	90	90	90
	Nickel Oxide	NiO	Hexagonal (Rh)	90	90	120
0.5 mol Ni (500°C)	Bunsenite, syn	NiO	Cubic	90	90	90
	Nickel Oxide	NiO	Hexagonal (Rh)	90	90	120
0.1 mol Ni (575°C)	Bunsenite, syn	NiO	Cubic	90	90	90
	Nickel Oxide	NiO	Hexagonal (Rh)	90	90	120
0.5 mol Ni (575°C)	Bunsenite, syn	NiO	Cubic	90	90	90
	Nickel Oxide	NiO	Hexagonal (Rh)	90	90	120
0.1 mol Ni (600°C)	Bunsenite, syn	NiO	Cubic	90	90	90
	Nickel Oxide	NiO	Hexagonal (Rh)	90	90	120
0.5 mol Ni (600°C)	Bunsenite, syn	NiO	Cubic	90	90	90
	Nickel Oxide	NiO	Hexagonal (Rh)	90	90	120

From XRD analysis, crystallite size can be calculated using Scherrer formula:

$$d = \frac{K\lambda}{\beta \cos \theta}$$

Where;

d = crystallite size;

$K = 0.9$;

λ = the wavelength of the diffraction peaks;

θ = the Bragg's angle at maximum peak

β = the full width of the XRD peak at half maximum intensity of the peak (FWHM)

The Scherrer equation predicts crystallite thickness if crystals are smaller than 1000Å. Broadening of a diffraction peak is expected to reflect some large scale feature in the crystal.

Table 4.2: Crystal Size for Sample 0.1 mol Ni

Sample Name	Calcination Temp(°C)	K	Wavelength(Å)	Obs. Max 2θ°	FWHM (2θ°)	Crystal size(nm)
0.1 mol Ni	300	0.9	1.5406	43.306	0.631	0.473
0.1 mol Ni	500	0.9	1.5406	43.355	0.876	0.341
0.1 mol Ni	575	0.9	1.5406	43.433	0.85	0.351
0.1 mol Ni	600	0.9	1.5406	43.53	0.855	0.349

Table 4.3: Crystal Size for Sample 0.5 mol Ni

Sample Name	Calcination Temp(°C)	K	Wavelength(Å)	Obs. Max 2θ°	FWHM (2θ°)	Crystal size(nm)
0.5 mol Ni	300	0.9	1.5406	43.369	0.423	0.706
0.5 mol Ni	500	0.9	1.5406	43.349	0.537	0.556
0.5 mol Ni	575	0.9	1.5406	43.342	0.424	0.704
0.5 mol Ni	600	0.9	1.5406	43.382	0.463	0.645

Figure 4.5: Graph of Crystal Size Respect to Calcinations Temperature

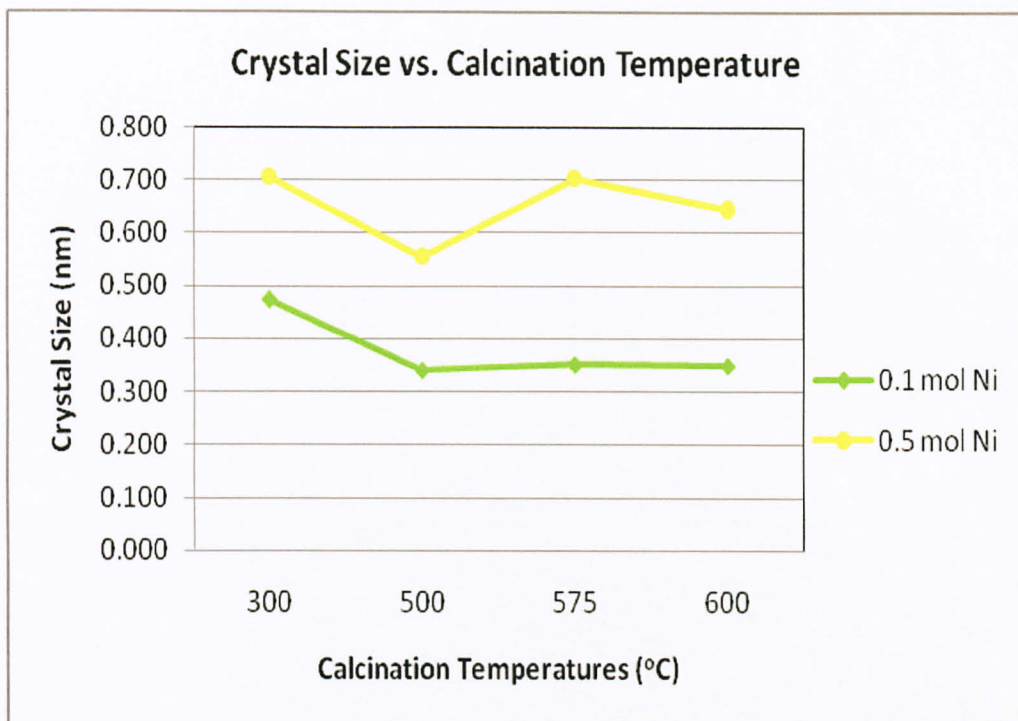
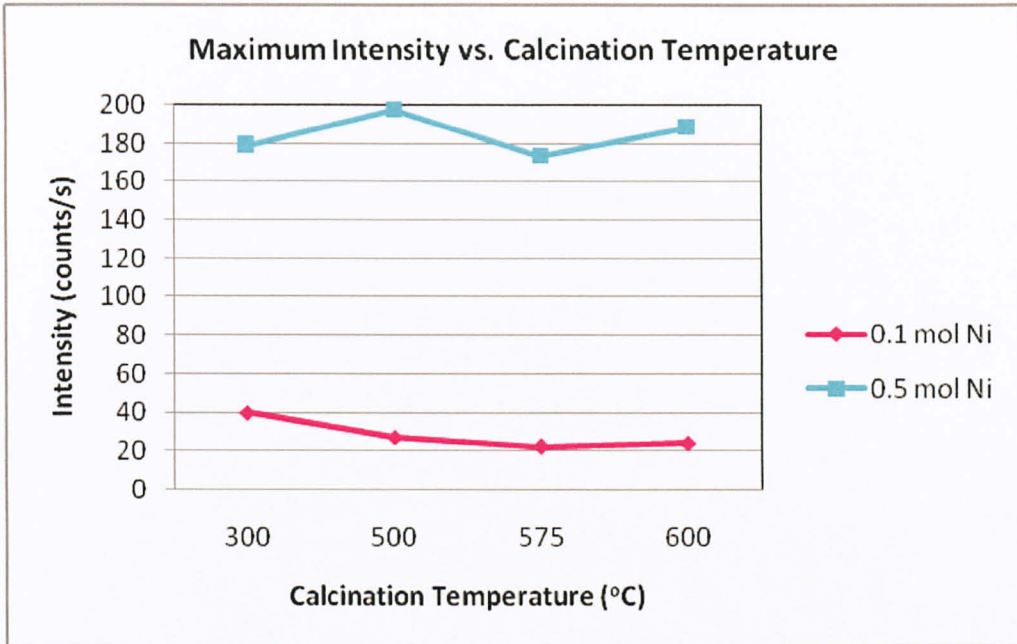


Table 4.4: Maximum Intensity Respect to Calcination Temperature

Sample Name	Calcination Temp(°C)	Max Intensity (Cps)
0.1 mol Ni	300	39.9
0.1 mol Ni	500	27.3
0.1 mol Ni	575	22.5
0.1 mol Ni	600	24.2

Sample Name	Calcination Temp(°C)	Max Intensity (Cps)
0.5 mol Ni	300	179
0.5 mol Ni	500	198
0.5 mol Ni	575	174
0.5 mol Ni	600	189

Figure 4.6: Graph of Maximum Intensity Respect to Calcinations Temperature



The intensity of each peak is caused by the crystallographic structure, the position of the atoms within the elementary cell and their thermal vibration. The line width and shape of the peaks may be derived from conditions of measuring and properties like particle size of the sample material (Basic in XRD@2001, Buker AXS).

From the Figure 4.5, the crystallite size increases as the temperature increases due to crystallite agglomerates. All the crystal sizes are below 100 nm where shows that the particles have met the nanoparticle size.

The grain growth and microstructure depend on many factors, such as the sintering/calcine temperature, stoichiometric, the amount and nature of the non-soluble constituents, the presence or otherwise of a liquid phase and the chemistry occurring within the grain during sintering. Since the preparation condition of this particular sample was inconsistent with others, the results become entirely different. Meanwhile, the decreasing trend of the crystallite size with increasing sintering temperature may due to rapid crystal growth at the beginning of sintering process that cause voids and the particles to grow together to form crystallite grains.

Scanning Electron Microscopy (SEM)

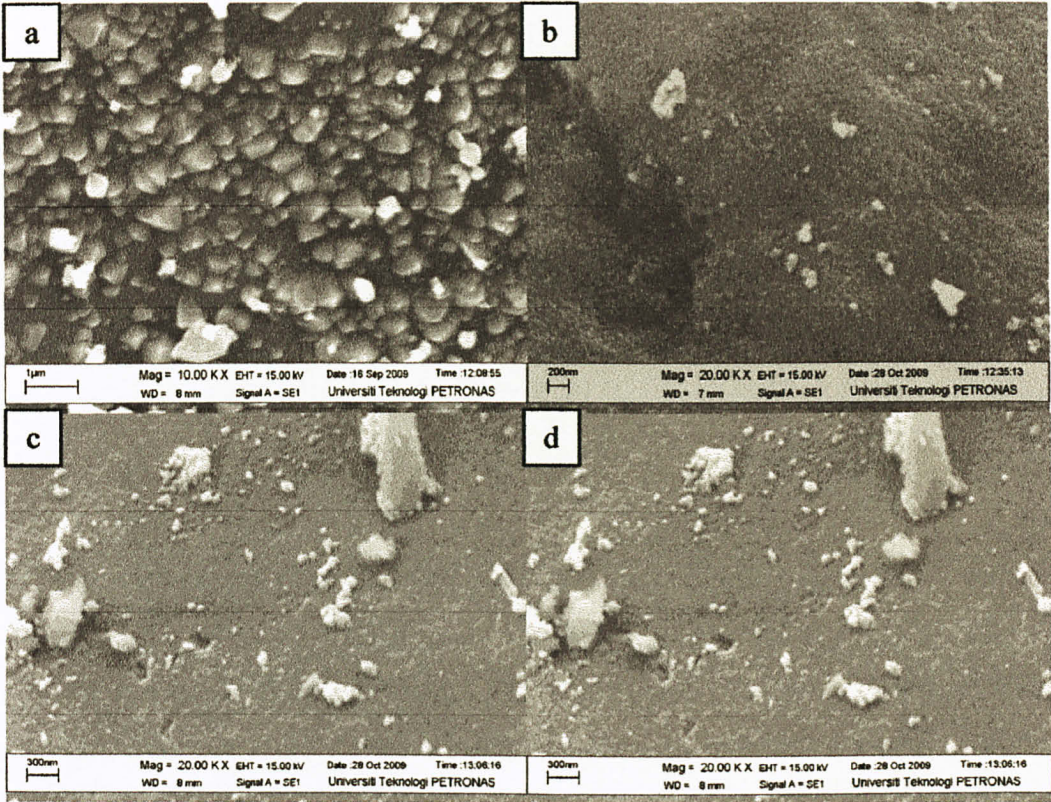


Figure 4.7: The morphology of Ni/SiO₂ for 0.1 mol (NO₃)₂.6H₂O at (a) 300°C, (b) 500°C, (c) 575°C and (d) 600°C

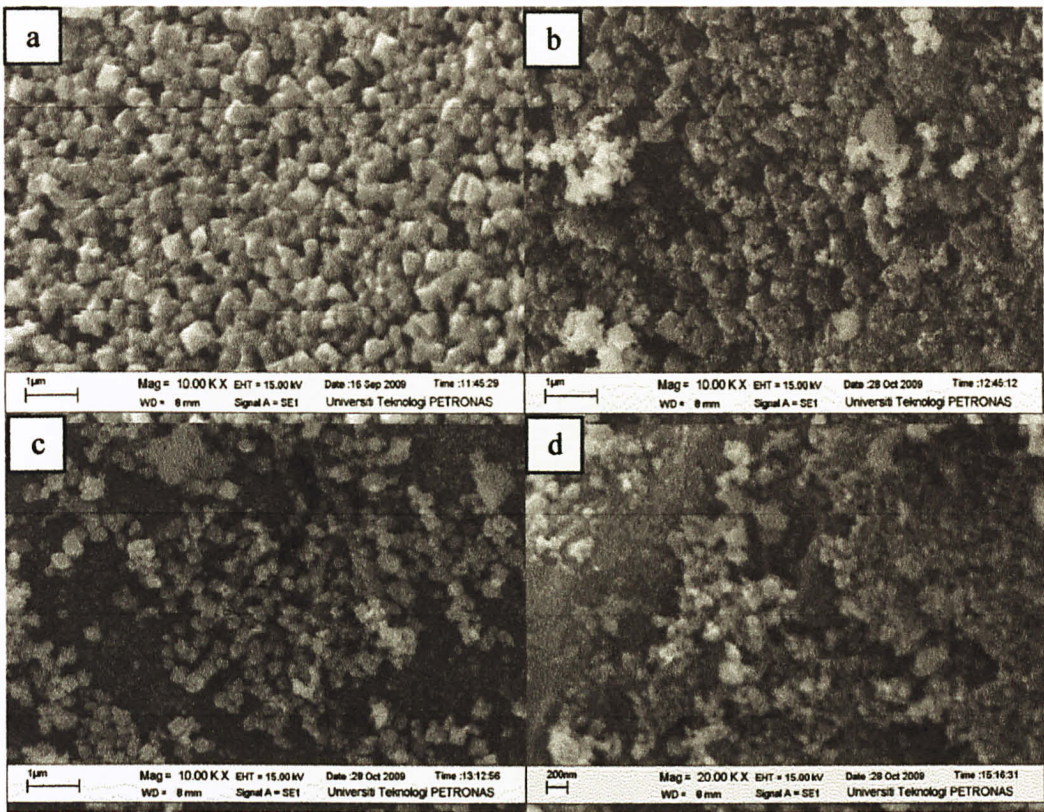


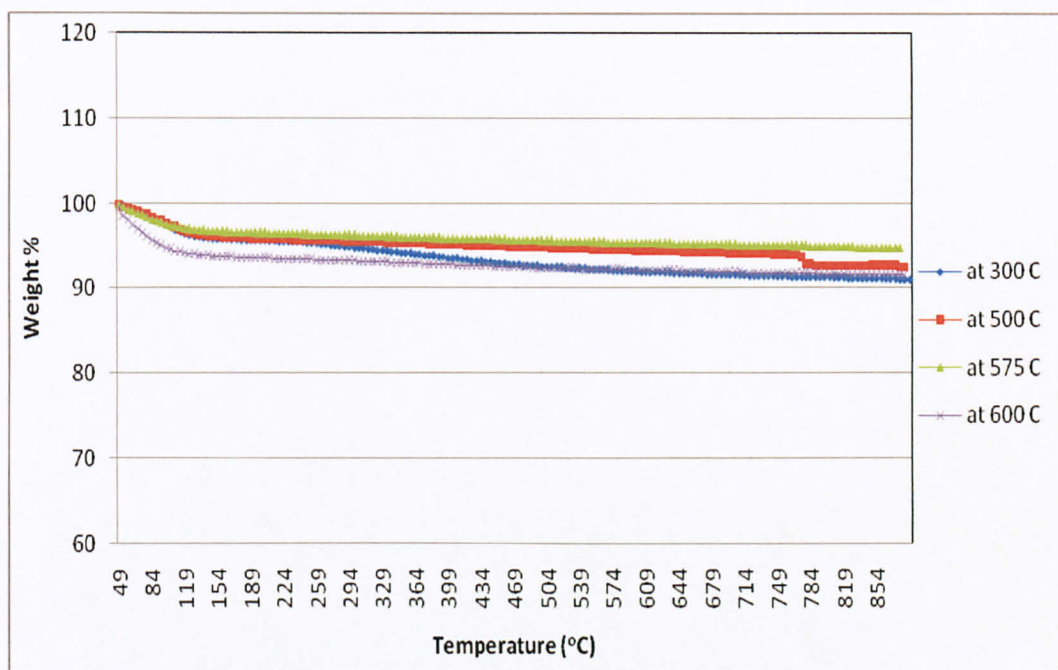
Figure 4.8: The morphology of NiO/SiO₂ for 0.5 mol (NO₃)₂.6H₂O at (a) 300°C, (b) 500°C, (c) 575°C and (d) 600 °C

One can observe that the grain boundaries are not well-defined for all the samples. This would be due to the sintering temperature not high enough for the complete formation of the microstructure. By increasing sintering temperature it can be seen from Figure 4.7 and Figure 4.8 that the microstructure of the particles becomes finer and porous but not well distributed.

Thermo Gravimetric Analysis (TGA)

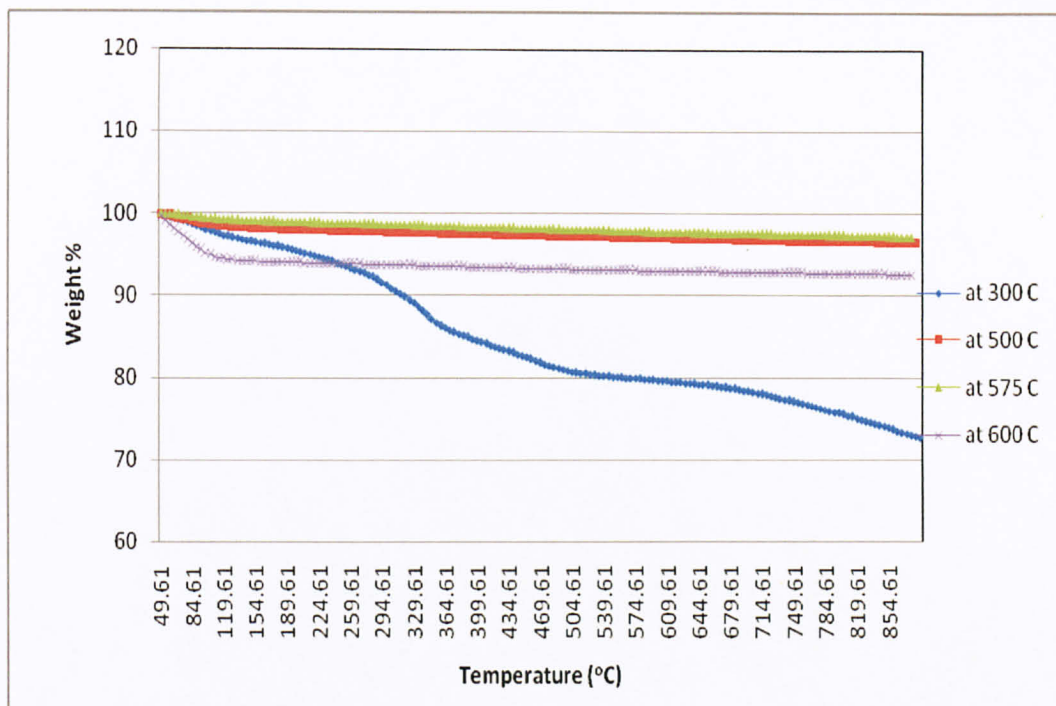
This testing is a type of testing that is performed on samples to determine changes in weight in relation to change in temperature. TGA normally is performed on dried samples to study and determine at what temperature the decomposition will occur. But, the Figure 4.9 and Figure 4.10 below show the analysis on calcine samples.

Figure 4.9: Graph of TGA Analysis for 0.1 mol Ni



The weight decreases between 50 – 120 °C for all samples would be elimination of moisture content in the samples. From the graph, after 120 °C not much weight loss occurs. So, it proves that all the organic groups such as hydroxyl group, carboxyl group and nitrate fully decompose after 6h calcination.

Figure 4.10: Graph for TGA Analysis for 0.5 mol Ni



The weight decreases between 50 – 120 °C for all samples would be elimination of moisture content in the samples. From the graph, after 120 °C not much weight loss occurs excluding for sample of 0.5 mol Ni at 300 °C. So, it proves that all the organic groups such as hydroxyl group, carboxyl group and nitrate fully decompose after 6h calcination. Gradual decomposition of the sample of 0.5 mol Ni at 300 °C which in blue line proceeds resulting in the gradual weight decrease starting from 120 °C until 900 °C. Temperature of 300 °C is not enough for 0.5 mol Ni composition to decompose all the organic groups.

Fourier Transform Infrared Spectroscopy (FTIR)

Fourier Transform Infrared Spectroscopy (FTIR) can provide very useful information about functional group. The technique can be used to analyze organic materials and some of inorganic materials based on how infrared radiations is absorbed by the target material, to produces an IR spectrum that can be used to identify functional groups and molecular structure in the sample. IR spectroscopy correlation table in Appendix A lists some general absorption peaks for common types of atomic bonds and functional groups.

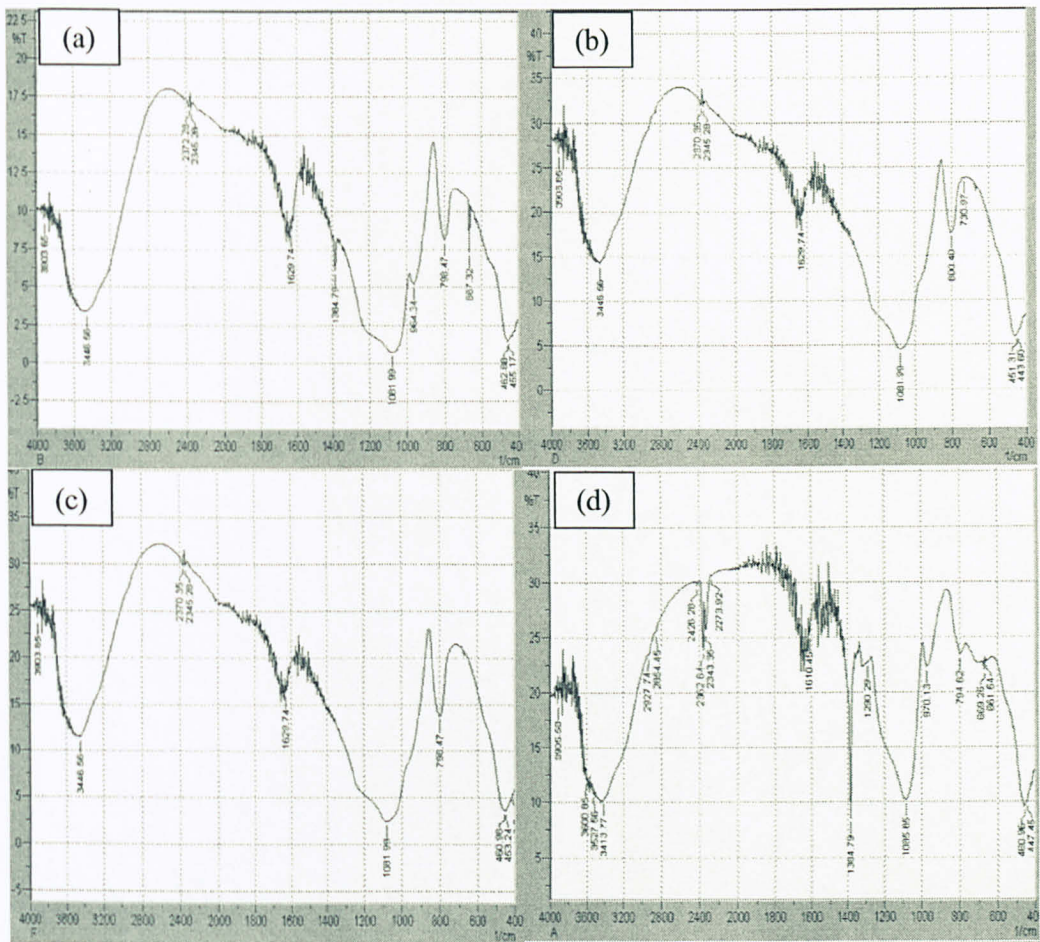


Figure 4.11: IR Spectra on Ni/SiO₂ for 0.1 mol Ni (a) 300°C, (b) 500 °C, (c) 575 °C, (d) 600 °C

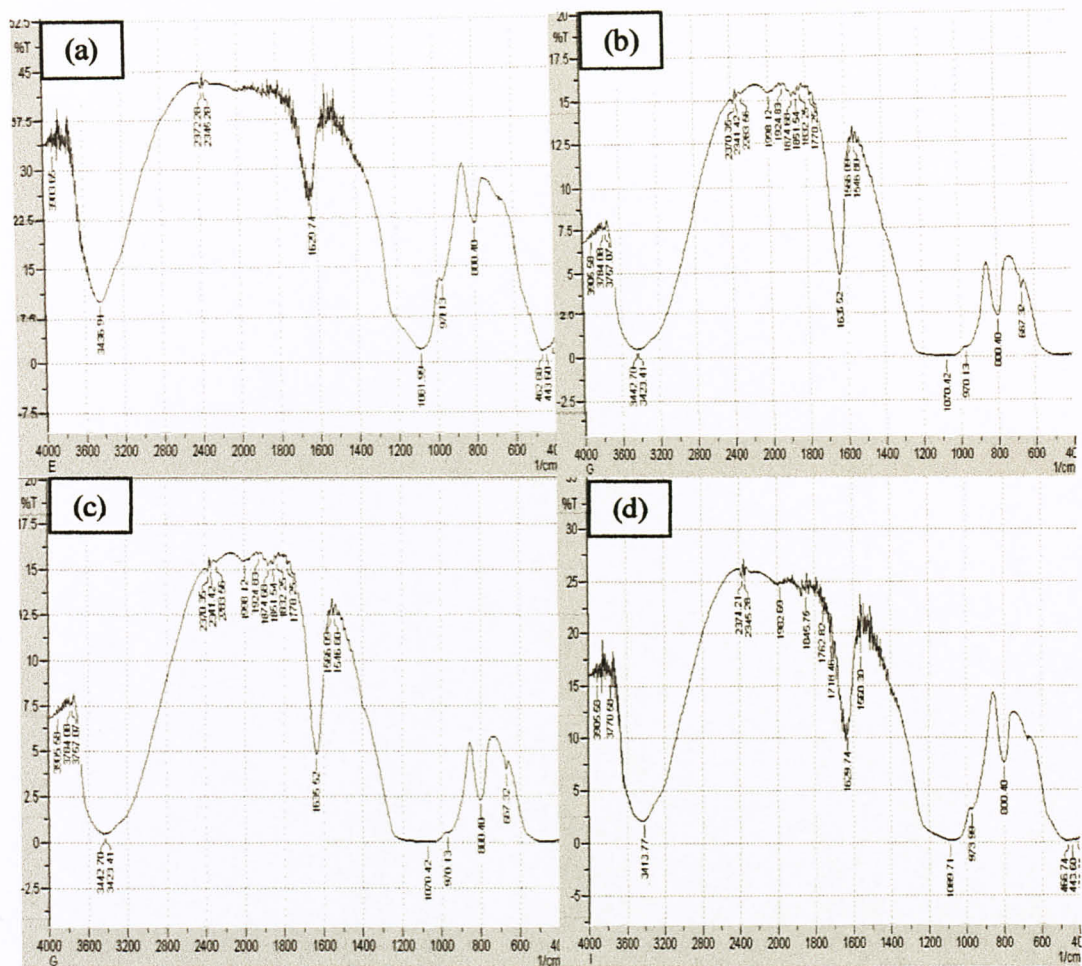


Figure 4.12: IR Spectra on Ni/SiO₂ for 0.5 mol Ni (a) 300°C, (b) 500°C, (c) 575°C, (d) 600°C

Table 4.5: Functional Groups of Compound

Frequencies (cm⁻¹)	Functional Groups	Bond
798.47	Silicon	Si-O-Si
800.40	Silicon	Si-O-Si
964.34	Silicon	Si-OH
1080.06	Carboxylic acid	C-OH
1081.99	Carboxylic acid	C-OH
1384.79	Nitrate	NO ₃ ⁻
2345.28	silane	Si-H
3446.56	alcohol	O-H
3448.49	alcohol	O-H

Frequencies (cm⁻¹)	Functional Groups	Bond
798.47	Silicon	Si-O-Si
800.40	Silicon	Si-O-Si
964.34	Silicon	Si-OH
970.13	Silicon	Si-OH
973.99	Silicon	Si-OH
1081.99	Carboxylic acid	C-OH
1384.79	Nitrate	NO ₃ ⁻
3436.91	alcohol	O-H
3446.56	alcohol	O-H

CHAPTER 5

CONCLUSION AND RECOMMENDATION

5.1 Conclusion

The sol gel synthesis provides suitable route for the preparation of small metal particles with narrow distribution and homogeneously distributed over the silica support. Nanoparticle is prepared by sol gel method which used an inorganic metal salt as a precursor. The characteristics of the nanoparticles are analyzed by XRD, FTIR, SEM, and TGA. The lowest crystal size of this Ni/SiO₂ is at 500°C. As increasing in sintering temperatures, the particles become finer and homogeneously distributed over the support. Porous structure of the silica matrix; number, shape and volume of the pores depends on amount of precursor salt. Many parameters and operational condition need to be tested which can influence the porous structure of silica and to obtain satisfactory results of nanoparticle.

5.2 Recommendation

- 1) Use organic additives for example citric acid to increase the formation of mesopores and increase in Ni dispersion [Takahashi et. al].
- 2) Further study will be conducted to utilize it for hydrogenation of oils
- 3) Repeat the experiment three or more times to get correct and accurate results
- 4) For correct data, do TGA analysis before and after calcination.
- 5) Analyze under Temperature Programmed Reduction (TPR) to get the information about total metal surface area

REFERENCES

1. Yi Liu, D.J. Sellmyer & Daisuke Shindo, *Handbook of Advanced Magnetic Materials*, Springer, 2006, Volume 1: Nanostructural Effects
2. B Cantor, *Novel Nanocrystalline Alloys and Magnetic Nanomaterials*, Institute of Physics, Series in Materials Science and Engineering, 2005
3. G. Piccaluga, A. Corrias, G. Ennas & A. Musinu, *Sol-gel Preparation and Characterization of Metal-Silica and Metal Oxide-Silica Nanocomposites*, Trans Tech Publications, Materials Science Foundation 13, 2000
4. B. Corain, G. Schmid & N. Toshima, *Metal Nanocluster in Catalysis and Materials Science*, ELSEVIER, The Issue of Size Control, 2008
5. Gian Paolo Chiusoli & Peter M Maitlis, *Metal-catalysis in Industrial Organic Process*, RSC Publishing, 2006
6. Sergey P. Gubin, *Magnetic Nanoparticles*, WILEY-VCH, 2009
7. Witold Lojkowski & John R. Blizzard, *Interfacial Effects and Novel Properties of Nanomaterials*, Scitec Publications, 2003
8. Tessy Maria Lopez, David Avnir & Michel Aegerter, *Emerging Fields in Sol-Gel Science and Technology*, Kluwer Academic Publishers, 2003
9. Carlo Perego & Pierluigi Villa, *Catalyst Preparation Methods*, ELSEVIER, *Journal of Catalysis Today*, Catalysis Today 34 (1997)
10. P. Muralidharan, I. Prakash, M. Venkateswarlu & N. Satyanarayana, *Sol-gel Synthesis and Structural Characterization of Nanocomposite Powder: NiAl₂O₄:SiO₂*, NSTI-Nanotech Vol. 3 (2004)

11. J. B. Laughlin, J. L. Sarquis, V. M. Jones & J. A. Cox, *Using Sol-Gel Chemistry to Synthesize a Material with Properties Suited for Chemical Sensing*, Journal of Chemical Education, Vol. 77 No. 1 January 2000
12. Abhishek Singh, *Magnetic Nano Particles --Fabrication, Analysis and Application*, MatE 297, SJSU Spring 2006
13. T. Ueckert, R. Lamber, N.I. Jaeger' & U. Schubert, *Strong metal support interactions in a Ni/SiO₂ catalyst prepared via sol-gel synthesis*, ELSEVIER, Applied Catalysis A: General 155 (1997) 75-85
14. O. Cherifi, M.M Bettahar & A. Auroux, *Microcalorimetric Study of the Acidity and Basicity of Ni/SiO₂ Catalysts Modified by Metallic Additive Fe, Co, Zr and Ce*, ELSEVIER, Thermochemica Acta 3006 (1997), 131 – 134
15. Ryoji Takahashi, Satoshi Sato, Toshiaki Sodesawa & Madoka Kato, *Preparation of Cu/SiO₂ Catalyst by Solution Exchange of Wet Silica Gel*, Kluwer Academic Publishers, Journal of Sol-gel Science and Technology 19 (2000), 715 – 718
16. Ryoji Takahashi, Satoshi Sato, Toshiaki Sodesawa, Masanori Suzuki & Nobuyuki Ichikuni, *Ni/SiO₂ Prepared by Sol-gel Process Using Citric Acid*, ELSEVIER, Microporous and Mesoporous Materials 66 (2003), 197 – 2008
17. C. J. Brinker and G. W. Sherer, "Sol-Gel Science", Academic Press, San Diego, 1990
18. M. Stefanescu, C. Caizer, M. Stoi, O. Stefanescu, *Ni, Zn/SiO₂ Ferrite Nanocomposites Prepared By An Improved Sol-gel Method and Their Characterisation*, Journal of Optoelectronics and Advanced Materials, Vol 7, NO. 2, April 2005, page 607-614

APPENDIX

(A) Infrared Spectroscopy

IR Absorptions for Representative Functional Groups

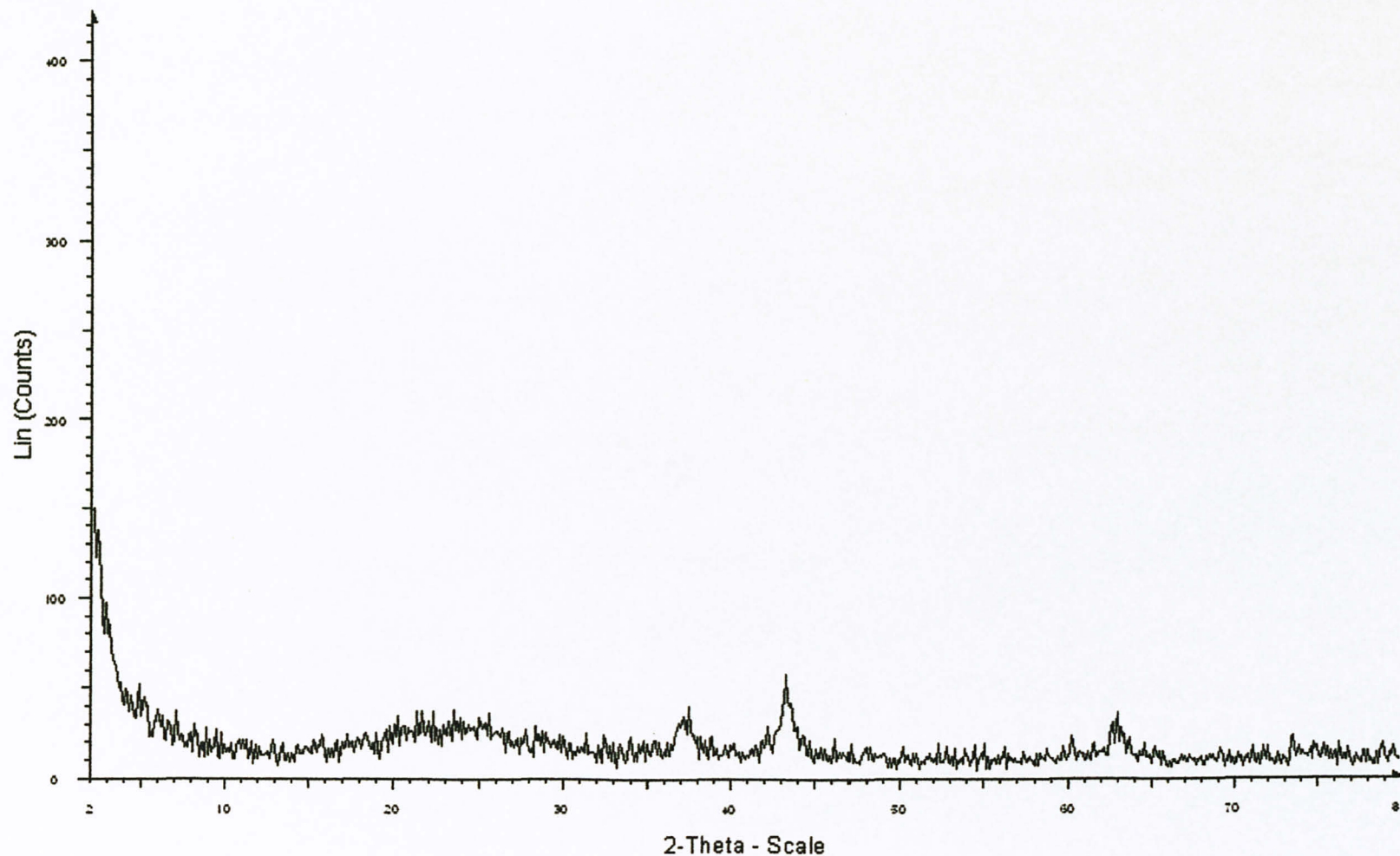
Functional Group	Molecular Motion	Wavenumber (cm ⁻¹)
alkanes	C-H stretch	2950-2800
	CH ₂ bend	~1465
	CH ₃ bend	~1375
	CH ₂ bend (4 or more)	~720
alkenes	=CH stretch	3100-3010
	C=C stretch (isolated)	1690-1630
	C=C stretch (conjugated)	1640-1610
	C-H in-plane bend	1430-1290
	C-H bend (monosubstituted)	~990 & ~910
	C-H bend (disubstituted - E)	~970
	C-H bend (disubstituted - 1,1)	~890
	C-H bend (disubstituted - Z)	~700
C-H bend (trisubstituted)	~815	
alkynes	acetylenic C-H stretch	~3300
	C,C triple bond stretch	~2150
	acetylenic C-H bend	650-600
aromatics	C-H stretch	3020-3000
	C=C stretch	~1600 & ~1475
	C-H bend (mono)	770-730 & 715-685
	C-H bend (ortho)	770-735
	C-H bend (meta)	~880 & ~780 & ~690
	C-H bend (para)	850-800
alcohols	O-H stretch	~3650 or 3400-3300
	C-O stretch	1260-1000

ethers	C-O-C stretch (dialkyl)	1300-1000
	C-O-C stretch (diaryl)	~1250 & ~1120
aldehydes	C-H aldehyde stretch	~2850 & ~2750
	C=O stretch	~1725
ketones	C=O stretch	~1715
	C-C stretch	1300-1100
carboxylic acids	O-H stretch	3400-2400
	C=O stretch	1730-1700
	C-O stretch	1320-1210
	O-H bend	1440-1400
esters	C=O stretch	1750-1735
	C-C(O)-C stretch (acetates)	1260-1230
	C-C(O)-C stretch (all others)	1210-1160
acid chlorides	C=O stretch	1810-1775
	C-Cl stretch	730-550
anhydrides	C=O stretch	1830-1800&1775-1740
	C-O stretch	1300-900
amines	N-H stretch (1 per N-H bond)	3500-3300
	N-H bend	1640-1500
	C-N Stretch (alkyl)	1200-1025
	C-N Stretch (aryl)	1360-1250
	N-H bend (oop)	~800
amides	N-H stretch	3500-3180
	C=O stretch	1680-1630
	N-H bend	1640-1550
	N-H bend (1°)	1570-1515
alkyl halides	C-F stretch	1400-1000
	C-Cl stretch	785-540
	C-Br stretch	650-510
	C-I stretch	600-485

nitriles	C,N triple bond stretch	~2250
isocyanates	-N=C=O stretch	~2270
isothiocyanates	-N=C=S stretch	~2125
imines	R ₂ C=N-R stretch	1690-1640
nitro groups	-NO ₂ (aliphatic)	1600-1530&1390-1300
	-NO ₂ (aromatic)	1550-1490&1355-1315
mercaptans	S-H stretch	~2550
sulfoxides	S=O stretch	~1050
sulfones	S=O stretch	~1300 & ~1150
sulfonates	S=O stretch	~1350 & ~11750
	S-O stretch	1000-750
phosphines	P-H stretch	2320-2270
	PH bend	1090-810
phosphine oxides	P=O	1210-1140

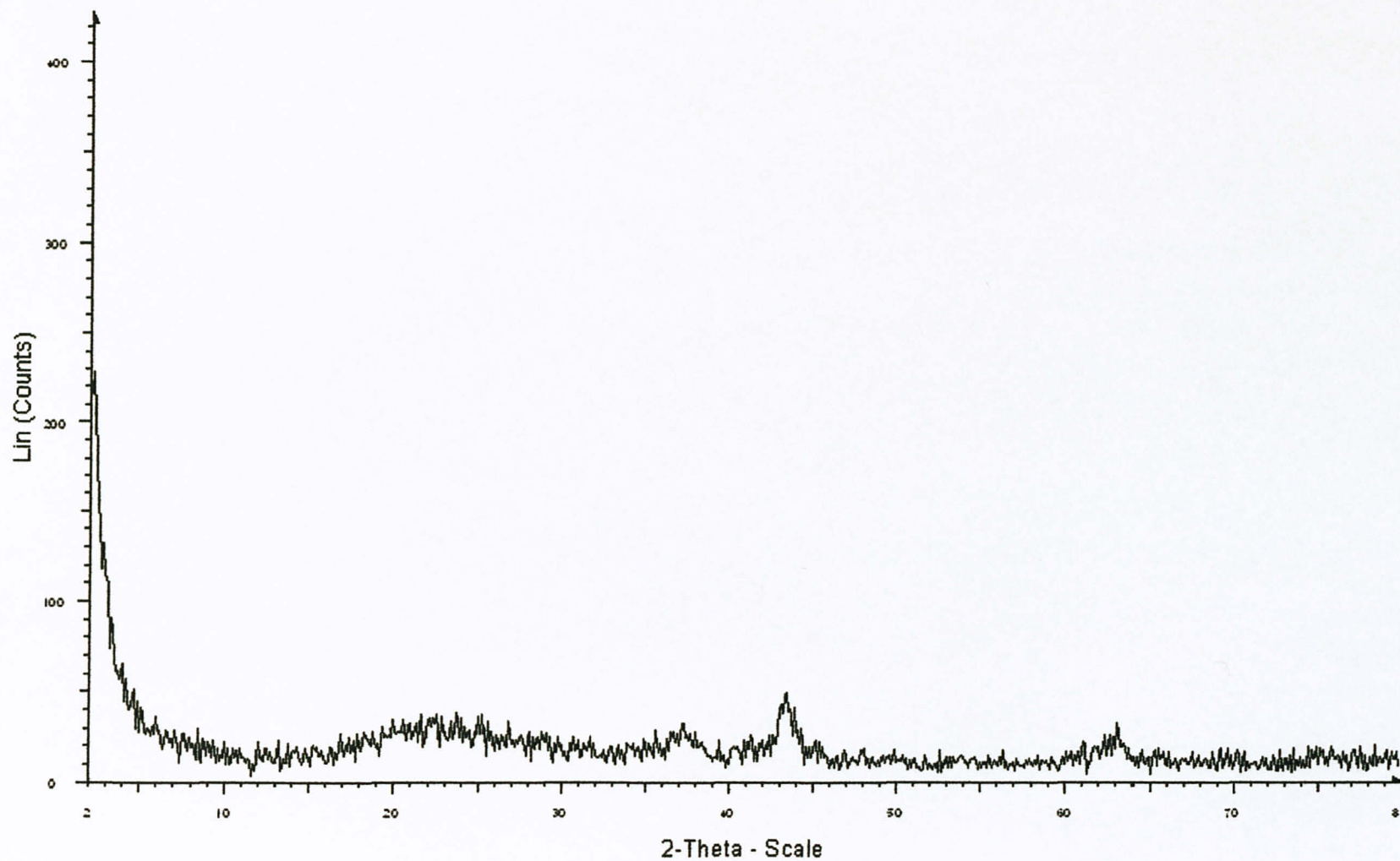
B: Individual XRD Diffractogram

(a) 0.1 mol Ni at 300°C



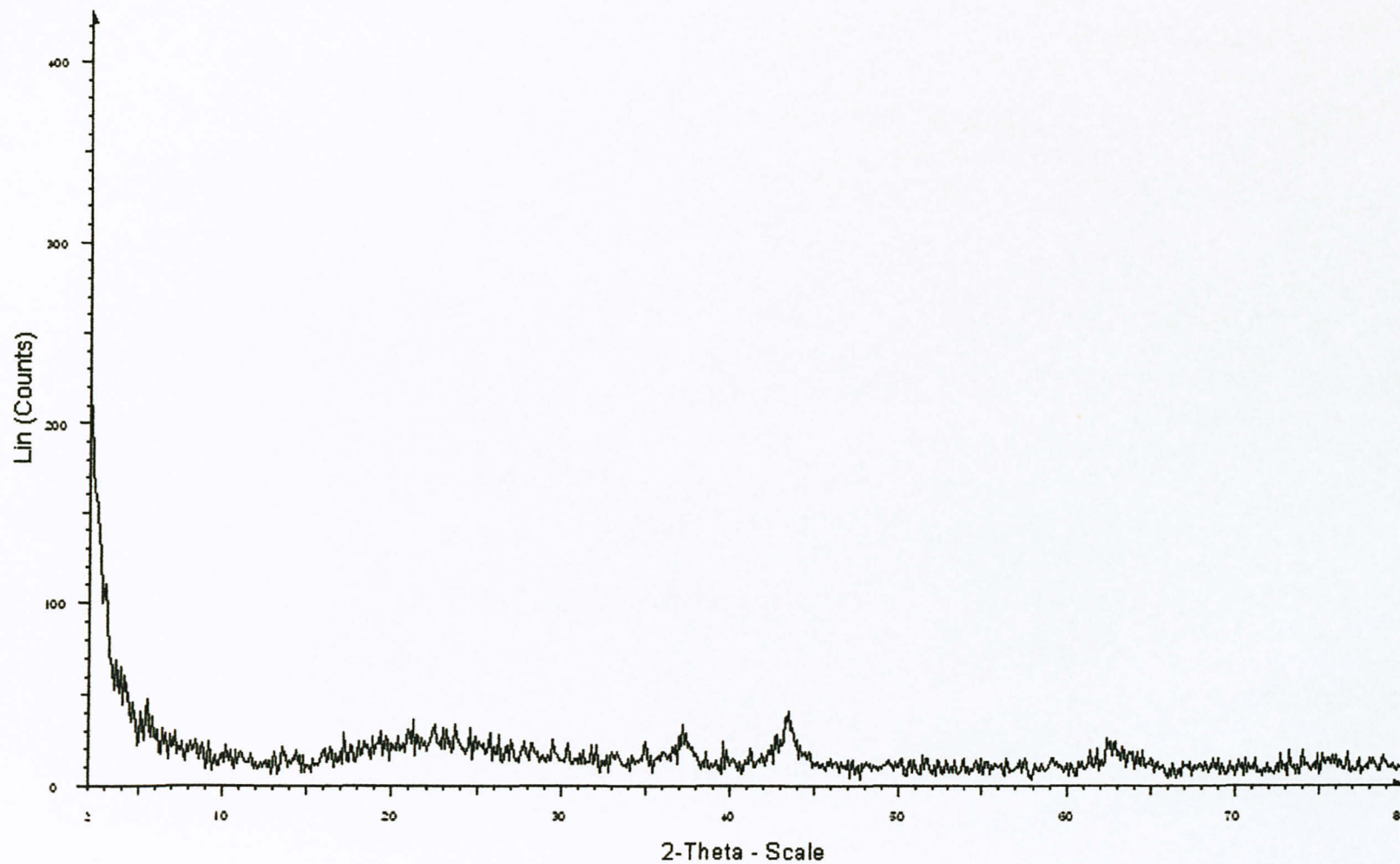
Sample 5 - File: Sample 5.raw - Type: 2 θ : θ locked - Start: 2.000 ° - End: 80.000 ° - Sep: 0.100 ° - Step time: 1. s - Temp.: 25 °C (Room) - Time Started: 1254892928 s - 2-Theta: 2.000 ° - Theta: 1.000 °
Operator: Import

(b) 0.1 mol Ni at 500°C



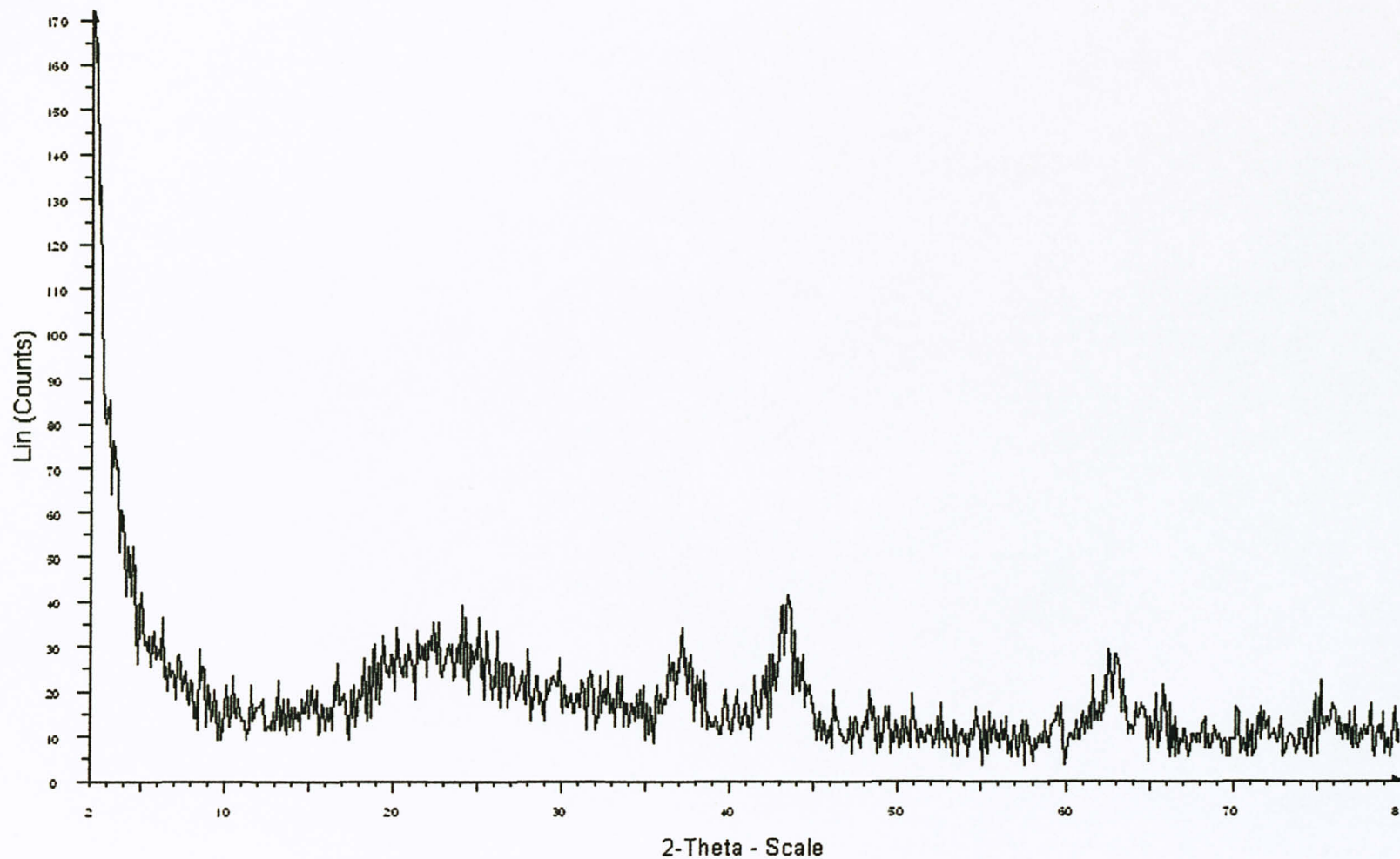
Sample D - File: Sample D.raw - Type: 2 θ / θ locked - Start: 2.000 ° - End: 80.000 ° - Step: 0.100 ° - Step time: 1. s - Temp: 25 °C (Room) - Time Started: 1254895232 s - 2-Theta: 2.000 ° - Theta: 1
Open ratio: 1:1

(c) 0.1 mol Ni at 575°C



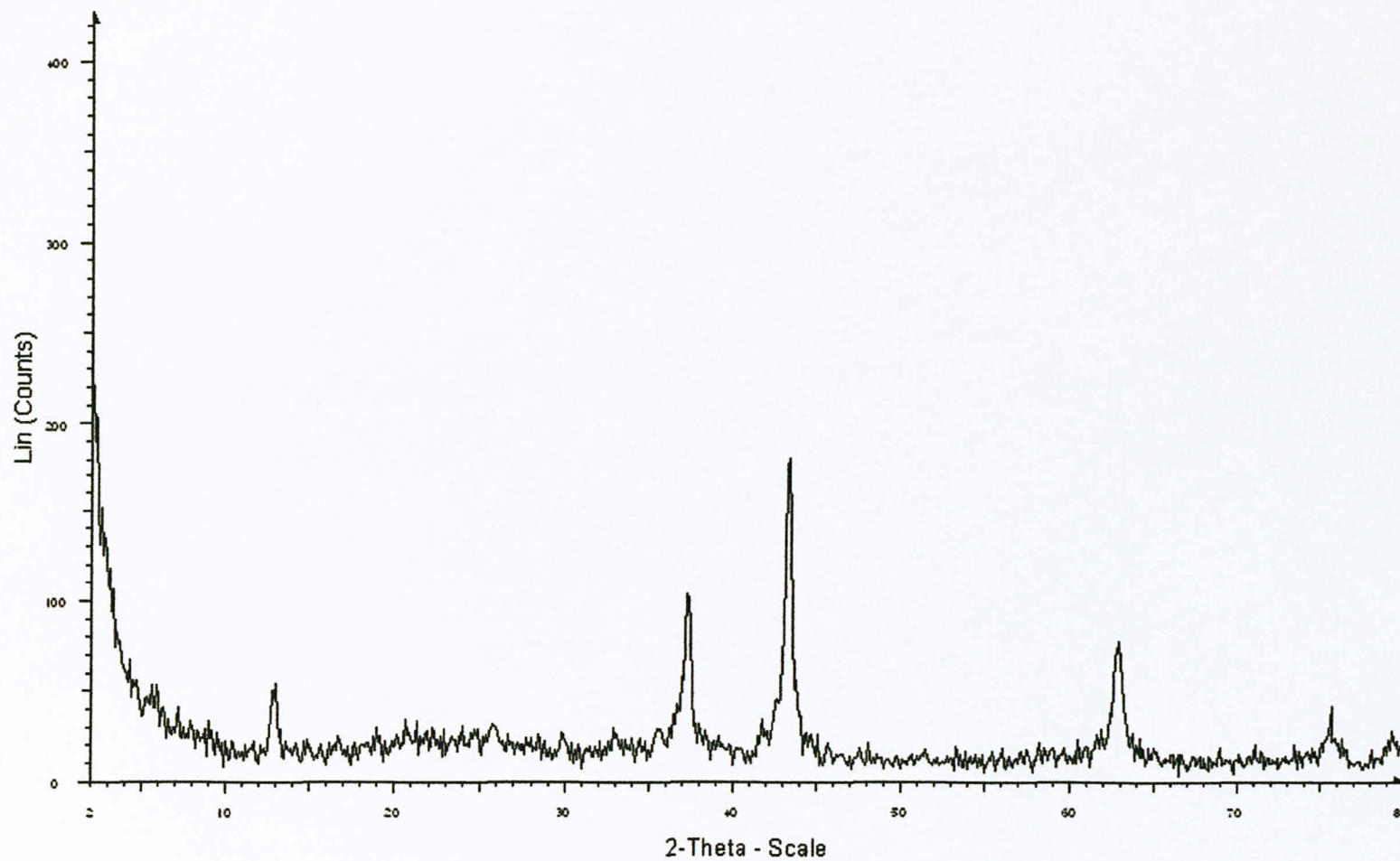
Sample F - File: Sample F.raw - Type: 2 θ / θ locked - Start: 2.000 ° - End: 80.000 ° - Step: 0.100 ° - Step time: 1. s - Temp.: 25 °C (Room) - Time Started: 1254897664 s - 2-Theta: 2.000 ° - Theta: 1.000 °
Operations: Import

(d) 0.1 mol Ni at 600°C



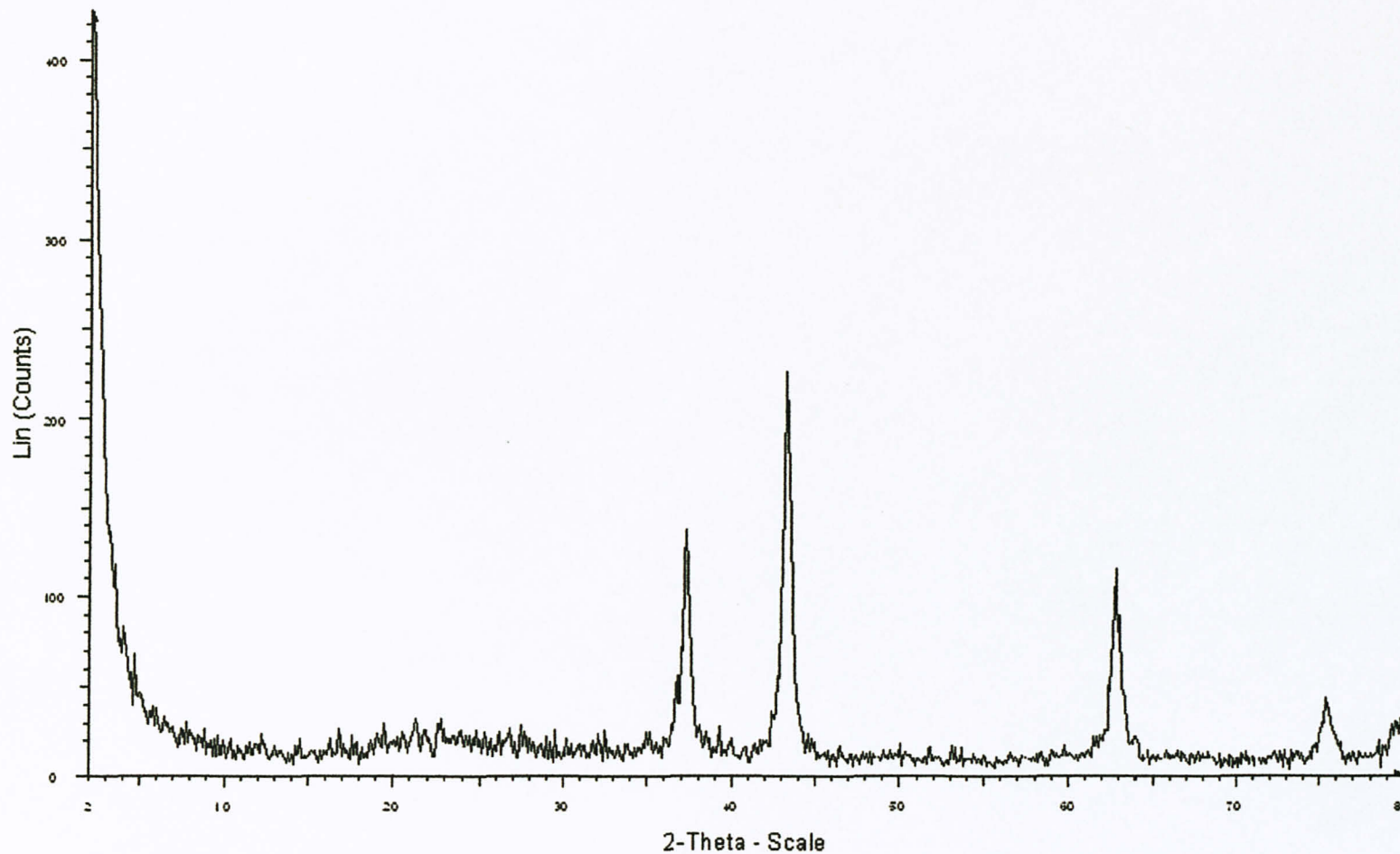
Sample H - File: Sample H.raw - Type: (2 θ / λ) locked - Start: 2.000 ° - End: 80.000 ° - Step: 0.100 ° - Step time: 1. s - Temp: 25 °C (Room) - Time Started: 1254960128 s - 2-Theta: 2.000 ° - Theta: 1
Operator: Import

(e) 0.5 mol Ni at 300°C



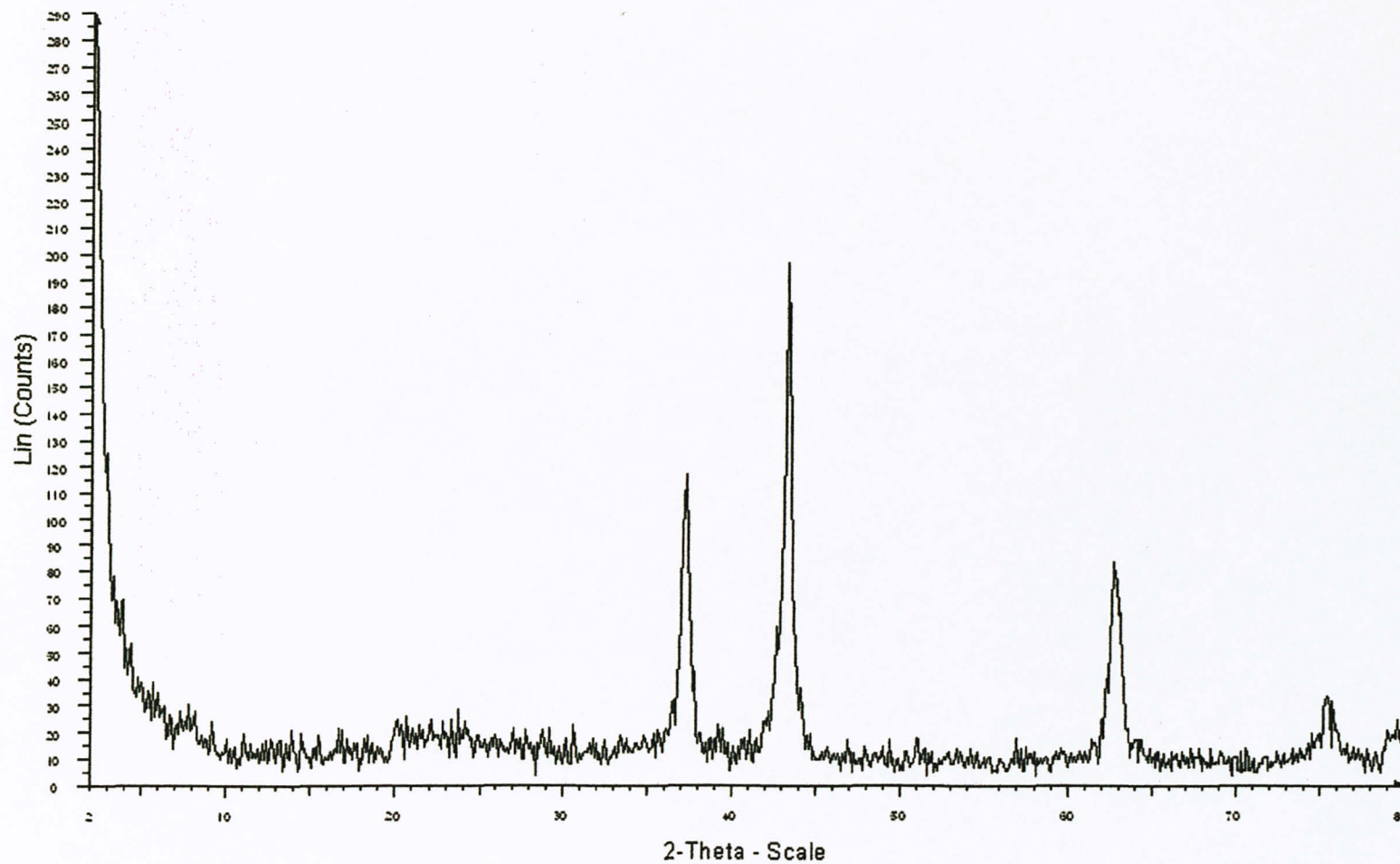
Sample A - File: Sample A.tgz - Type: 2Th:Ti locked - Start: 2.000 ° - End: 80.000 ° - Step: 0.100 ° - Step time: 1. s - Temp.: 25 °C (Room) - Time Started: 1251866528 s - 2-Theta: 2.000 ° - Theta: 1.000 ° - Operator: Import

(f) 0.5 mol Ni at 500°C



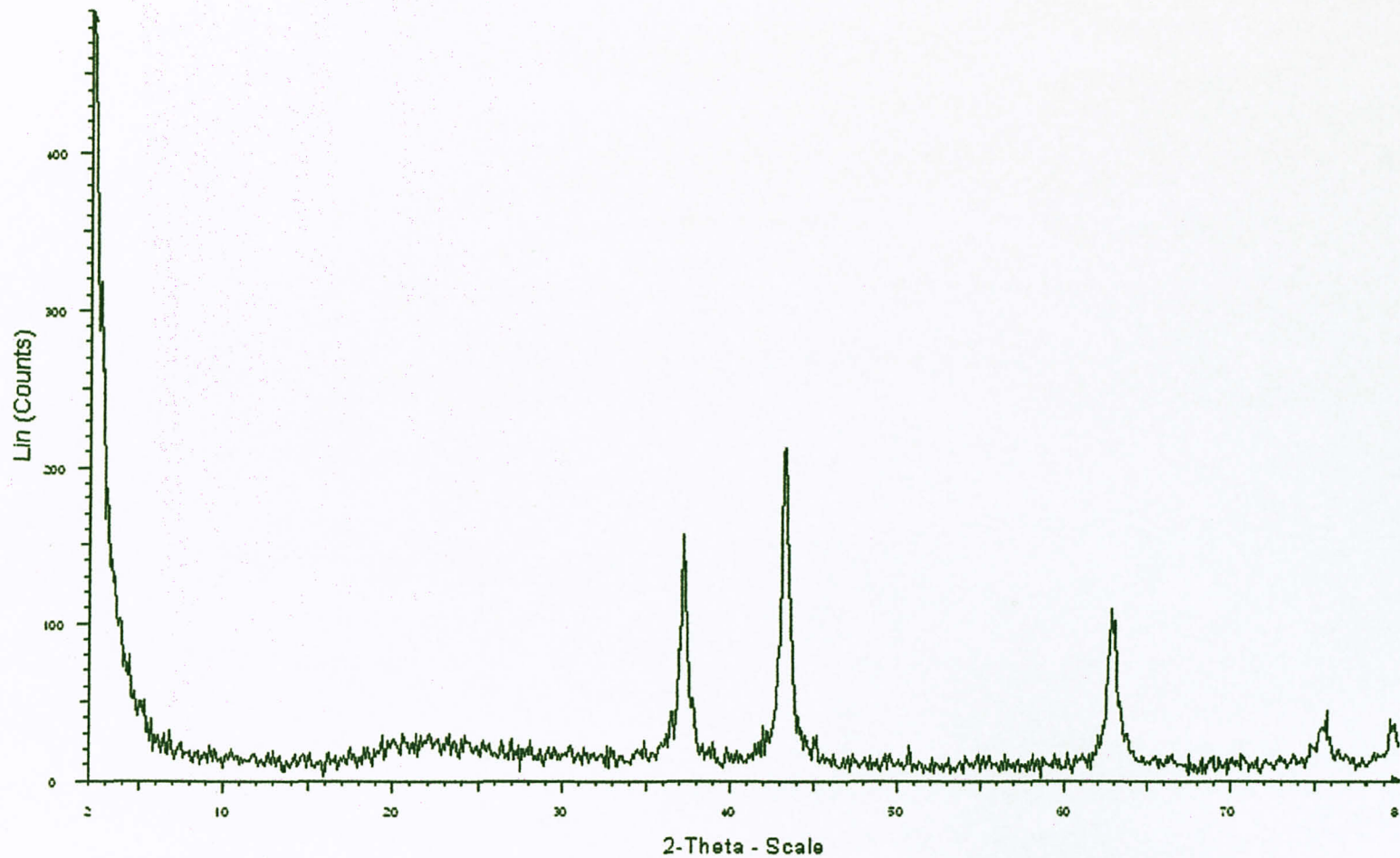
Sample E - File: Sample E.raw - Type: 2 θ / θ locked - Start: 2.000 ° - End: 80.000 ° - Step: 0.100 ° - Step time: 1. s - Temp: 125 °C (Room) - Time Started: 1251896640 s - 2-Theta: 2.000 ° - Theta: 1.000 ° - Operator: Import

(g) 0.5mol Ni at 575°C



Sample G - File: Sample G.raw - Type: CT/TL locked - Start: 2.000 ° - End: 80.000 ° - Step: 0.100 ° - Step time: 1. s - Temp.: 25 °C (Room) - Time Started: 1231907006 s - 2-Theta: 2.000 ° - Theta: 1
Operation: Import

(h) 0.5mol Ni at 600°C



Sample 1 - File: Sample 1.aux - Type: 2Th/Th indexed - Start: 2.000 ° - End: 80.000 ° - Step: 0.100 ° - Step time: 1. s - Temp.: 25 °C (Room) - Time Started: 1251962304 s - 2-Theta: 2.000 ° - Theta: 1.0
Operations: Import